Distribution Category:
Physics—General (UC-34)

ANL-83-24

ANL--83-24

DE84 011428

ARGONNE NATIONAL LABORATORY
9700 South Cass Avenue
Argonne, Illinois 60439

THE OPTICAL PROPERTIES AND COMPLEX DIELECTRIC FUNCTION OF METALLIC ALUMINUM FROM 0.04 TO 10^4 eV

by

D. Y. Smith and E. Shiles*
Materials Science and Technology

and

M. Inokuti
Environmental Research Division

March 1983

*Present address: Gulf Research and Development Co.
Houston, Texas 77236

TABLE OF CONTENTS

Page

ABSTRACT..1

I. GENERAL FEATURES...1

A. Intraband Spectrum.......................................2

B. Interband Spectrum.......................................4

II. OPTICAL MEASUREMENTS AND SAMPLE CONDITIONS..............9

A. Polished Polycrystalline Samples.........................9

B. Thin-Film Polycrystalline Samples........................9

1. Surface Oxide Layers....................................10
2. Bulk Inclusion of Residual Gas 11
3. Surface Roughness.......................................12

C. Noncrystalline and Liquid Samples.......................12

III. OPTICAL CONSTANTS AND DATA ANALYSIS...................14

A. Room-Temperature Optical Constants......................14

B. Room-Temperature Dielectric Function and Reflectance......17

C. Temperature Dependence..................................21

Appendix A, Optical Constants of Aluminum, 0.039-75 eV.........23

Appendix B, Dielectric Function of Aluminum (Short Form).......31

Appendix C, Dielectric Function and Optical Properties of Aluminum 0.04-10^4eV (Long Form)........................35

ACKNOWLEDGMENTS..48

REFERENCES 48

LIST OF FIGURES

No.	Title	Page
1.	Extinction Coefficient for Metallic Aluminum at Room Temperature	3
2.	Reflectance of Metallic Aluminum at Room Temperature	6
3.	The Interband Conductivity of Metallic Aluminum	7
4.	The Complex Refractive Index of Metallic Aluminum	16
5.	The Complex Dielectric Function of Metallic Aluminum	18
6.	The Reflectance of Metallic Aluminum	20
7.	The Phase of the Reflectivity of Metallic Aluminum	21
8.	The Optical Conductivity of Clean, Polycrystalline Aluminum Films	22

LIST OF TABLES

	Title	Page
I.	Drude Parameters for Metallic Aluminum	5
II.	Optical Constants of Aluminum, 0.039 - 75 eV	25
III.	Dielectric Function of Aluminum (Short Form)	32
IV.	Dielectric Function and Optical Properties of Aluminum 0.04 - 10^4 eV (Long Form)	36

THE OPTICAL PROPERTIES AND COMPLEX DIELECTRIC FUNCTION OF METALLIC ALUMINUM FROM 0.04 to 10^4 eV

by

D. Y. Smith, E. Shiles, and M. Inokuti

ABSTRACT

Measurements of the optical properties of metallic aluminum are reviewed and available data are analyzed to obtain the bulk values of the optical constants and the complex dielectric function from 0.04 eV to 10 keV. The intra- and interband contributions to the dielectric function are discussed briefly, and recently proposed values for the Drude parameters describing the intraband absorption are critically considered. Factors influencing experimental measurements are discussed with emphasis on sample properties such as surface oxide layers, bulk inclusion of gases, surface roughness, and degree of crystallinity. The results of recent optical measurements are tabulated, along with recommended values of the optical properties resulting from a self-consistent Kramers-Kronig analysis of reflectance, transmission, and electron-energy-loss studies. The tabular data include the complex dielectric function, the complex index of refraction, and the reflectance and phase shift for normal incidence on a smooth, oxide-free surface. Detailed tabulations are given for the infrared, visible, and ultraviolet regions of the spectrum.

I. GENERAL FEATURES

Metallic aluminum is one of the most widely measured and analyzed materials[1-7] with regard to optical properties. These properties are dominated by three practically nonoverlapping groups of electronic transitions corresponding to absorptions by conduction-band, L-shell, and K-shell electrons. Figure 1 shows the absorption spectrum for the crystalline solid.

The 3 electrons/atom (e/a) donated to the conduction band by the atomic $3s^2 3p$ valence levels give rise to a typical metallic absorption from zero to ~15 eV, the bulk plasmon energy, $\hbar\omega_p$. In crystalline samples, this portion of the spectrum is dominated by intraband transitions in the far infared and by two strong interband absorptions at ~0.5 eV ($\lambda \approx 2.5$ μm) and ~1.5 eV ($\lambda \approx 0.8$ μm). The higher-energy interband transition is evident as a small peak in the absorption spectrum of Fig. 1, but the lower-energy transition is obscured by the strong intraband absorption. In the noncrystalline or partially crystalline solid and in the liquid state, the interband spectrum is strongly modified or absent (see Sec. IIC).

A. Intraband Spectrum

The intraband contribution to the optical properties may be described phenomenologically to within experimental error with a Drude-model dielectric function[8] for the electron gas,

$$\varepsilon_{Drude} = \varepsilon_0 - \frac{\Omega_p^{\,2}}{\omega(\omega + i/\tau)}, \tag{1}$$

where the contribution to the dielectric function from core interband transitions has been included in ε_0. Here Ω_p is the (phenomenological) plasma frequency for intraband transitions, and τ is the intraband relaxation time. The quantity ε_0 is effectively constant throughout the region of conduction-electron absorption (that is, to well above the plasma frequency) with a value[7] of 1.03_5.

In addition to using the quantity Ω_p, the strength of the intraband transitions is commonly expressed in terms of the effective number density of electrons participating in intraband transitions

$$n_{eff,intraband} = \frac{m_e \Omega_p^2}{4\pi e^2} . \tag{2}$$

Here m_e and e are the free-electron mass and charge, respectively. A second alternative is the optical mass defined by[8]

$$m_{opt} = m_e \;\frac{n_c}{n_{eff,intraband}} , \tag{3}$$

where n_c is the density of conduction elections.

Similarly, the intraband relaxation time is often given in terms of the damping coefficient

$$\gamma = \tau^{-1} . \tag{4}$$

A quantity frequently cited for comparison with electrical experiments is the dc conductivity in the Drude model

$$\sigma(0) = \frac{\Omega_p^{\,2}}{4\pi\gamma} . \tag{5}$$

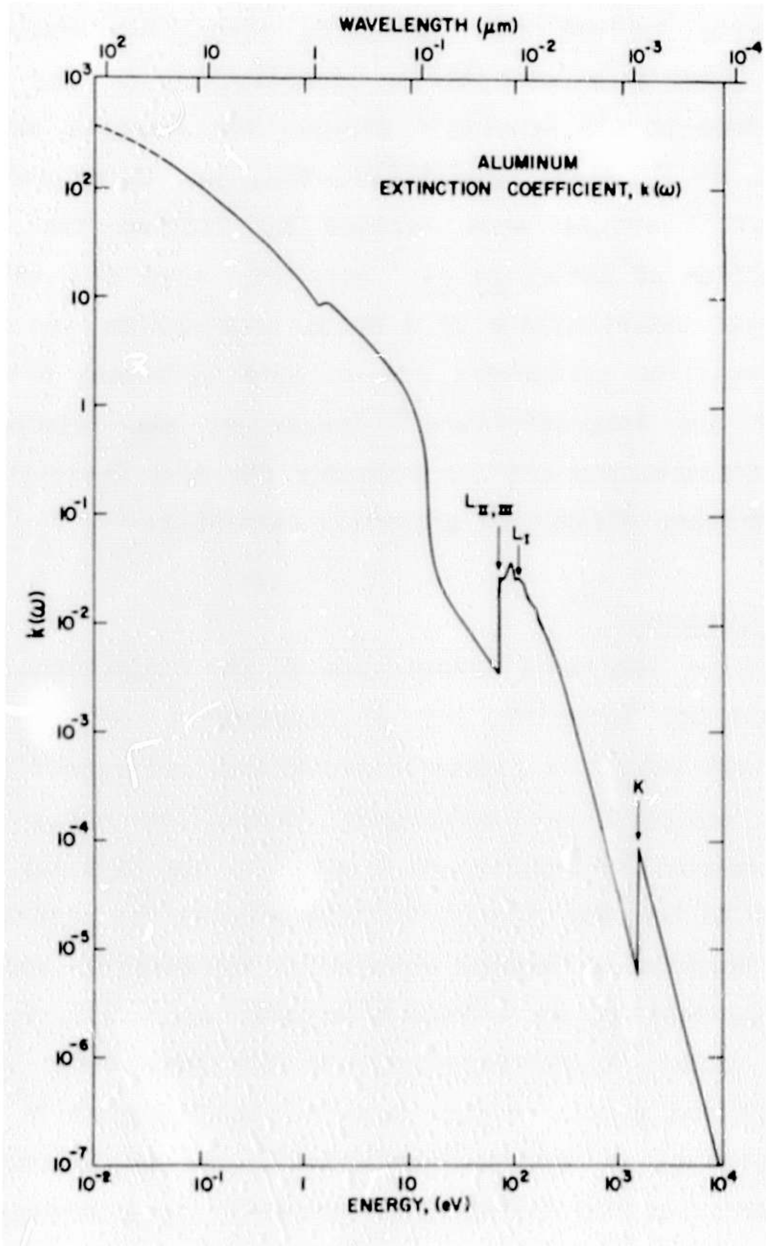

Fig. 1. The Extinction Coefficient (i.e., the imaginary part of the refractive index) for Metallic Aluminum at Room Temperature. After Shiles et al. (Ref. 7).

A variety of fits of Eq. 1 have been made to infrared data for polycrystalline samples of aluminum,[1,3,5,9-14] but early work was incomplete because the interband transitions at ~0.5 and ~1.5 eV were not always reckoned with. Table I gives some of the more recent determinations of the Drude parameters and the experimental bulk dc conductivity. The "0.5-eV" interband transition was not accounted for by Ehrenreich _et al._[1] or by Powell,[3] so that their Drude terms include some interband absorption strength, as well as damping. This leads to a conductivity significantly smaller than the measured bulk value. Bennett and Bennett[11] assumed the measured value of $\sigma(0)$, but also neglected the "0.5-eV" transition; this led to an overestimate of Ω_p. The Smith-Segall[14] values were derived by fitting the reflectance-based dielectric function of Shiles et al.[7] over the range of 0.04-3.0 eV, assuming it to be a linear superposition of a Drude term and the two interband transitions. The resulting parameters are in good agreement with the Mathewson-Myers[5] fit of the Ashcroft-Sturm[15] theory of the interband spectrum to ellipsometric measurements and are probably the best description of the room-temperature intraband absorption presently available.

B. Interband Spectrum

The two strong interband transitions of the conduction-electron spectrum in the crystalline material are a consequence of the "parallel-band" effect[1,15-17] that occurs in almost-free-electron polyvalent metals. In these materials the occupied and unoccupied conduction bands are effectively parallel over substantial regions of k space in the vicinity of high-symmetry planes parallel to the zone faces. Allowed transitions between these parallel bands lead to prominent interband absorptions at energies approximately twice the Fourier component of the effective crystal potential, $V_{\vec{K}}$, for the reciprocal lattice vector, $\vec{K}$, corresponding to the zone face in question. In aluminum, absorption between almost-parallel bands occurs in the neighborhood of surfaces parallel to the hexagonal (111) and to the square (200) zone faces. The corresponding energy gaps predicted by a two-band model[15] using parameters[18] derived from de Haas-van Alphen measurements are $2V_{111} = 0.487$ eV and $2V_{200} = 1.53$ eV. The parallel-band absorption shows sharp rises near these energies followed by long tails toward higher energies, which join smoothly onto the band-to-band absorption arising from the remainder of the Brillouin zone.[15,17] In addition, theory predicts[19,20] an accidental degeneracy of the energy bands leading to a weak, but finite interband absorption down to zero energy. However, this has not been verified experimentally because the interband component is overwhelmed by the intraband absorption below a few tenths of an electron volt.

The 1.5-eV (0.8-μm) interband absorption is readily apparent as a pronounced drop in the reflectance for crystalline samples (Fig. 2) and as a

Table I. Drude parameters for the intraband absorption of metallic aluminum (see Eqs. 1-5 in the text). The effective density of electrons, n_{eff}, is given in electrons per atom (e/a); in aluminum the actual density of conduction electrons is 3 e/a.

		Strength			Damping		dc Conductivity[a]	
Source	Temp (K)	$\hbar\Omega_p$ (eV)	n_{eff} (e/a)	m_{opt} (m_e)	τ (10^{-14} sec)	$\hbar\gamma = \hbar\tau^{-1}$ (meV)	$\sigma(0)$ (10^{17} sec^{-1}) Optical	Electrical
Ehrenreich et al. (1963), Ref. 1	RT	12.7	1.94	1.55	0.512	129	1.52	3.18^c - 3.28^d
Bennett et al. (1966)[b], Ref. 11	RT	14.7	2.60	1.15	0.801	82.2	3.18 (input)	
Powell (1970), Ref. 3	RT	12.2	1.80	1.67	0.66	100	1.81	
Dresselhaus et al. (1971), Ref. 12	RT	12.9 ± 0.7	2.0 ± 0.2	1.5 ∓ 0.2	0.5 ± 0.2	160 ∓ 60	1.60 ± 0.8	
Mathewson and Meyers (1972), Ref. 5	198	12.8	1.99	1.51	1.18	55.8	3.58	5.49^e
"	298	13.0	2.03	1.48	1.02	64.5	3.14	3.21^e
"	404	13.2	2.10	1.43	0.62	105	1.96	2.3^e
"	552	13.3	2.13	1.41	0.52	128	1.65	1.63^e
Benbow and Lynch (1975), Ref. 13	4.2	12.7	1.94	1.55	1.10	60	3.25	-
Smith and Segall (1981), Ref. 14	RT	12.5 ± 0.3	1.88 ± 0.09	1.60 ∓ 0.08	1.13 ± 0.05	58.5 ∓ 3.0	3.25 ± 0.3	3.18^c - 3.28^d

[a]The optical conductivity at $\omega = 0$ has been calculated from Eq. 5; the electrical values of $\sigma(0)$ are for dc measurements on bulk samples.

[b]$\sigma(0)$ was used as an input.

[c]Ref. 124.

[d]Ref. 125.

[e]Ref. 5.

small peak in the extinction coefficient (Fig. 1). Strong[21] appears to have first reported the former and Schultz[22] the latter. Ehrenreich et al.,[1] and Shklyarevskii and Yarovaya[23] identified the absorption responsible for these features as an interband transition.

The Drude absorption almost completely hides the second major interband absorption at ~0.5 eV. There is a suggestion of this interband transition in the early infrared measurements of Beattie[24] and in a slight change of slope

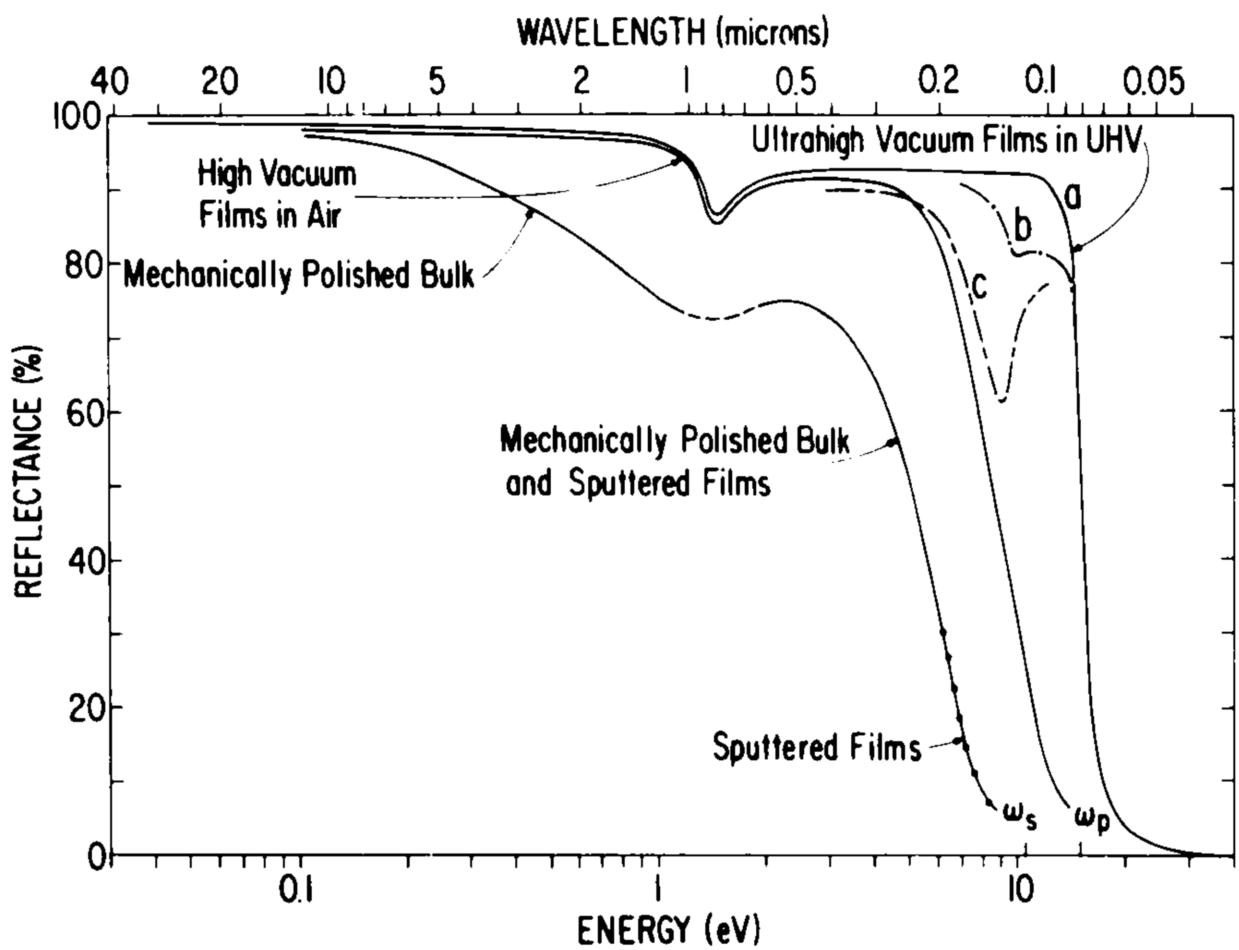

Fig. 2. The Reflectance of Metallic Aluminum at Room Temperature. Curve a applies to opaque, optically smooth, evaporated aluminum films prepared in uhv. The effect of light scattering and surface plasmons (at $\hbar\omega_s$ = 10.6 eV) is shown by curves b and c. Curve b was reported by Vehse et al. (Ref. 82) for a film on a clean microscope slide. Curve c was given by Endriz and Spicer (Ref. 48) for a uhv film with rms surface roughness of 18 Å. The "high-vacuum" curve is an average for films evaporated in vacua of the order of 10^{-5} Torr, for which surface and bulk oxidation occurs. The properties of such films vary widely, especially in the UV, presumably because of surface roughness. The lowest curve is representative of mechanically polished samples, but the reported range of measurements for these is extremely large. Data for sputtered films are available well into the UV; curiously they track the data for polished samples very closely at high energies.

in the ultrahigh-vacuum (uhv) reflectance data of Bennett et al. (see Figure 2 of Ref. 7). This transition was first definitively observed in low-temperature absorptivity experiments by Bos and Lynch.[26] Figure 3 shows the Bos-Lynch results for 4.2 K along with a separation of the room-temperature data by Smith and Segall[14] in terms of the real part of the interband conductivity

$$\sigma_{\text{interband}}(\omega) = \frac{-i\omega}{4\pi}\left[\varepsilon(\omega) - \varepsilon_{\text{Drude}}(\omega)\right] . \qquad (6)$$

Below about 0.3 eV the uncertainty in the experimental data and in the Drude parameters is so large that the interband contribution cannot be determined reliably from the available measurements.

Note the shift of the interband absorption toward higher energies as the temperature is lowered. Mathewson and Myer[5] studied this in detail for the "1.5-V" transition (see also Fig. 8).

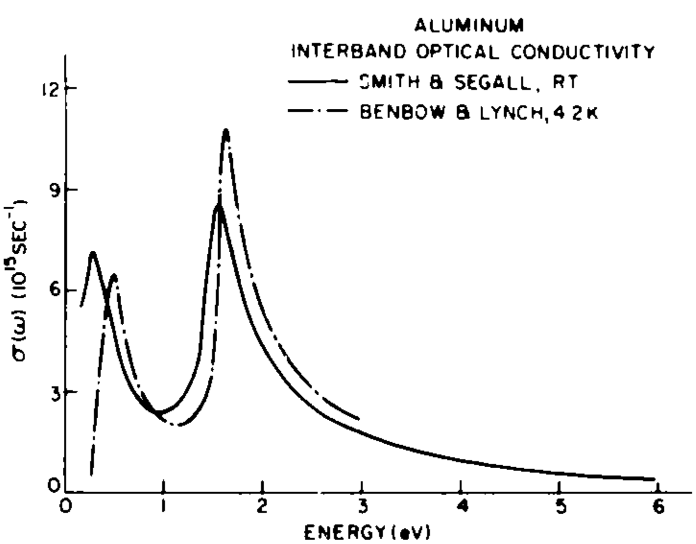

Fig. 3. The Interband Conductivity of Metallic Aluminum (real part). These values were obtained by subtracting the intraband contribution in the Drude model from the measured optical conductivity. The solid curve is for room temperature and was calculated by Smith and Segall (Ref. 14) who used Shiles et al.'s analysis of uhv reflectance data (Ref. 7). The dashed curve is taken from Benbow and Lynch (Ref. 13) and applies to electropolished samples at 4.2 K.

At low temperatures (~20 K), a weak fine structure is superimposed on the tail of the "1.5-eV" absorption in the range 2-2.5 eV.[27] Part of this structure appears to arise[14] from transitions near the corners of the Brillouin zone in the vicinity of the intersections of the two groups of planes responsible for the two strong parallel-band absorptions. Along these lines of intersection three bands are almost parallel with band gaps determined by both V_{200} and V_{111}. However, the transitions arising from these triplets of parallel bands are not as prominent as those associated with the doublet of parallel bands in the planes because of the smaller volume of k-space involved in the neighborhood of the lines of intersection. The result is two weak absorptions, one near the strong "0.5-eV" interband transition and the second just above the strong "1.5-eV" transition. These have been predicted in detail by band-structure calculations.[20,27]

II. OPTICAL MEASUREMENTS AND SAMPLE CONDITIONS

A. Polished Polycrystalline Samples

Quincke[28] began serious studies of the optical properties of aluminum in 1874. Early measurements were made on polished bulk or rolled samples.[28-35] Even though bulk aluminum takes a "high polish," it always retains a "hazy white surface"[31] and has a reflectance well below that of an uncontaminated evaporated film. As will become apparent, this is presumably the result of both scattering and absorption by the microscopically rough, oxide-coated surface. Figure 2 gives a composite of reflectance data for polished surfaces. The curve generally follows the data of Coblentz (IR),[31] Luckiesh (vis. + UV),[33] Quincke (vis.),[28] and Wulff (vis. + UV).[35] The polished-bulk-metal data are strongly affected by surface contamination and light scattering, particularly at shorter wavelengths. In the visible, Nutting[30] reports reflectance values ~10% higher than those shown, while values measured by Coblentz and Stair[34] are 10% lower. Taylor[36] gives an even more dramatic range and quotes reflectances from 33% (mill finish) to 84% (electropolished) at 296.7 nm.

B. Thin-Film Polycrystalline Samples

The key factor in obtaining accurate values of the optical properties was the discovery that aluminum could be sputtered[37] or evaporated[38] to form highly reflecting metal films. Early sputtered films were "brilliant."[39,40] However, evaporation by the tungsten-coil method[41,42] has become the preferred technique for sample preparation because of the method's high speed and potential for low contamination. The major impetus for these developments was the production of interferometer[41] and telescope[21] mirrors. (The superior reflectance of evaporated aluminum films over silver at short wavelengths extended stellar spectroscopy some 250 Å into the violet.)

Evaporated films show reflectances much higher than polished surfaces, particularly in the ultraviolet. Generally, the higher the vacuum and the faster the evaporation, the higher the reflectance.[43-46] Two curves for evaporated surfaces are shown in Fig. 2. The upper is for unoxidized, smooth films produced in ultrahigh vacuum (10^{-9}-10^{-10} Torr); the other is for films evaporated in conventional high vacuum (~10^{-5} Torr). The first is believed to correspond to a smooth, uncontaminated aluminum surface. The second is for more-or-less contaminated surfaces having oxide coating with no special attempts made to eliminate surface roughness. The uhv curve generally follows the data of Bennett et al.,[25] Hass and Waylonis[46] (although these were not uhv films, a high evaporation rate was used; this method has been shown to yield the same results as uhv preparation[47]), and Endriz and Spicer.[48] Beyond 11.8 eV the curve follows the analysis of Shiles et al.,[7] which relies heavily on electron energy-loss measurements[49] near ω_p, and on transmission and reflectance data of Ditchburn and Freeman[50] and x-ray absorption measurements[51] beyond ω_p.

The high-vacuum curve generally follows the data of Beattie,[10] Strong,[21] Hass,[43,52] Sabine,[53] Banning,[54] and Walker et al.[55] The curve shown is in close agreement from 250 to 2500 nm with the U.S. NBS reference standard first-surface aluminum mirror #2003a,[56] which has an aged oxide coating. The curve also generally has the same reflectance from 200 to 2000 nm as commercially available evaporated mirrors.[57] Films evaporated under higher vacuum or at high deposition rates generally have reflectances between the high-vacuum and uhv curves shown.[58] Values of the reflectance for oxide-free uhv and oxidized high-vacuum films shown in Figure 2 are given in Appendix A at the end of this report.

The differences between the various evaporated film data arise from surface oxide layers,[43,59-63] residual gas incorporated in the film,[44,45] surface roughness,[48,64,65] and film morphology.[47,66-68] These factors will be discussed briefly.

1. Surface oxide layers. A layer of Al_2O_3 forms rapidly on an aluminum surface, even in high vacuum.[69,70] The layer is both adherent and relatively impervious so that, once formed, it protects the underlying metal from further oxidation.[71] The thickness of the surface layer and its composition depends strongly on sample structure and history, particularly on chemical treatment.[21,47,66,68,71,72] Polarimetric studies of evaporated films simply exposed to the atmosphere indicate that the surface oxide layer is 20-55 Å thick,[45,59-63] but that thicker layers readily form in moist environments.[71] The surface layers are probably hydrated to varying degrees depending on the circumstances of formation. Preparation conditions,[43,47,73] purity,[73]

structure,[66,68] partial oxidation in vacuum before exposure to the atmosphere,[62] etc., all influence the reported thickness. In addition, exposure of aluminum surfaces in air to ultraviolet light has been found to decrease reflectance at short wavelengths; this is attributable to an increase in the oxidation rate of the surface.[43,66,73]

The oxide of aluminum is highly transparent from about 6 μm (0.2 eV)[74] to 180 nm (6.8 eV)[6,75] so that a surface oxide film does not decrease the reflectance significantly over this range. Moreover, in the infrared a light wave does not "see" the film.[43] (The incident and reflected electric waves must be out of phase by about π to create the required node in the electric field at the metal surface. Thus, provided the oxide thickness is much less than the wavelength of light, the electric fields of the incident and reflected waves almost cancel in the oxide layer, and coupling to the layer is negligible.) However, at the shorter wavelengths of the vacuum ultraviolet, the oxide layer has a strong effect. For example, at 121.6 nm (~ 10 eV) an oxide layer 17 Å thick decreases the reflectance by a factor of two.[60,73] Overcoatings of materials such as MgF_2 and LiF have been developed to preserve the reflectance of aluminum at short wavelengths by preventing the growth of oxide films.[43,76]

2. <u>Bulk inclusion of residual gas.</u> Studies of films evaporated at different rates and pressures indicate that the optical constants are very sensitive to residual gas incorporated into the bulk of the films,[44,45] specifically to the film composition within the penetration depth.[45] This is generally attributed[43-45,77] to oxide formation arising from the gettering of molecular oxygen or to the reduction of water vapor to form Al_2O_3 and hydrogen. The relevant parameter appears to be the ratio of the residual-gas pressure to the deposition rate, which is a measure of the arrival rate of residual-gas molecules to that of aluminum atoms.[44,45] Films deposited from high-purity starting material at terminal pressure/rate ratios of the order 10^{-8}- 10^{-9} Torr min Å^{-1} or less[45] have similar reflectances and appear to be uncontaminated for the purpose of optical property measurements, provided subsequent oxide formation is avoided.

The presence of surface effects has also been demonstrated in x-ray absorption measurements in the neighborhood of the L edge.[78,79] This has not been investigated in detail, but it has been associated with an apparent systematic overestimate of the L-shell absorption.[7]

3. Surface roughness. An extremely important factor in determining the bulk optical constants, particularly in the ultraviolet, is the roughness of the sample surfaces.[48,64,65] Surface roughness causes both scattering[80] and coupling to surface plasmons[81] (the latter lie at a frequency of $\hbar\omega_p/\sqrt{2} \approx 10.6$ eV for an aluminum-vacuum interface). Figure 2 shows reflectance curves for two low-contamination films[48,82,83] with a slight surface roughness for comparison with the smooth, uhv surface reflectance. The main reflectance drop lies near the surface-plasmon frequency, but the drop extends well into the visible, largely as a result of scattering. Even a slight surface roughness produces dramatic effects. For example, a film with an rms surface roughness of only 27 Å is reported[48] to exhibit a reflectance drop of 20% at 3 eV (400 nm). These effects account for the wide variation of reflectance previously found in the UV and often attributed to contamination.

C. Noncrystalline and Liquid Samples

Vapor-quenched solid and liquid aluminum exhibit typical metallic properties, but with a wide range of modifications in the interband spectrum. In the liquid state, aluminum exhibits no interband structure.[84] Rather, the conduction electron absorption appears to follow a free-electron Drude model to within experimental error. This is in agreement with the expectation that in the liquid state there is no long-range order and, hence, no well-defined band structure and Brillouin-zone boundaries.[85]

Similar properties might be anticipated for samples with a low degree of crystallinity. However, the optical spectrum of vapor-quenched aluminum films deposited at low temperature exhibits a complex behavior.[5,86] Films deposited at 25, 140 and 198 K show a progressive reduction in the intensity of the 1.5-eV interband absorption with decreasing substrate temperature. Essentially no 1.5-eV absorption remains in films deposited at 25 K.[86] The reduced 1.5-eV absorption does not show a shift in position or broadening, only a decrease in magnitude. Further, annealing of the films at room temperature restores the 1.5-eV absorption. These observations have been interpreted[5] to indicate that deposition from the vapor on a cooled substrate yields a two-phase system which is partly crystalline and partly amorphous, but which crystallizes on annealing.

This explanation cannot be complete since it is not consistent with analysis[86] of the 25 K films: these films show no 1.5-eV interband component and consequently would be considered to be noncrystalline in this interpretation. However, the optical properties are not described by the Drude model as those of the liquid can be. Rather, the conduction-electron absorption appears to consist of a Drude term plus a residual absorption near 0.5 eV, which is attributed to interband transitions characteristic of the $2V_{111}$ energy gap. A possible explanation[86] is that the film consists of small-diameter, close-packed planar clusters with characteristic (111) translational symmetry, but lacking the (200) translational symmetry of bulk aluminum.

III. OPTICAL CONSTANTS AND DATA ANALYSIS

A. Room-Temperature Optical Constants

The most reliable optical data presently available are for uncontaminated polycrystalline aluminum films prepared in ultrahigh vacuum. Measurements generally are made of reflectance at room temperature (18-25°C) and are now available over the range 0.04-11.8 eV (32 μm-105 nm)[25,48]. In addition, a number of ellipsometric studies[5,62,68,87,88] of thin films in the near IR and visible have recently become available, particularly through the studies of Mathewson and Myers[5,87] and of Liljenvall et al.[88] (The former also includes high- and low-temperature measurements.) Studies[13,26] of bulk electropolished polycrystalline and single-crystal samples have also been reported, but absolute optical properties were not measured. The results are, however, consistent with absolute measurements on thin films.

Ellipsometric measurements yield the optical constants directly, but reflectance measurements at normal incidence must be analyzed using dispersion theory. This has recently been done over a wide spectral range for the room-temperature uhv reflectance measurements by Shiles et al.[7] using a self-consistent Kramers-Kronig analysis. This involved combining the reflectance measurements below 11.8 eV with

(1) Electron-energy-loss measurements in the vicinity of the plasma frequency, and
(2) Transmission and angular-variation-of-reflectance measurements in the extreme UV and x-ray regions.

The energy-loss measurements were mainly those of Gibbons et al.[49] The higher-energy optical data were taken primarily from Ditchburn and Freeman,[50] Haensel et al.,[89] Gähwiller and Brown,[90] Fomichiev et al.,[91-93] Singer,[94] Ershov et al.,[95,96] Cooke and Stewardson,[97] Bearden,[98] Henke et al.,[99,100] Singman,[101] Lublin et al.,[102] Hubbel et al.,[103] and Davisson.[104] These high-energy data were for room temperature, but were not for uhv samples and may suffer from surface effects to some degree, particularly in the transmission measurements on thin films near the $L_{II,III}$ edge[78,79] and to a lesser degree between the plasmon energy and the $L_{II,III}$ edge (see below).

Since the Kramers-Kronig relations require knowledge of one optical function over the entire spectrum, the analysis proceeded by successive approximations. A trial reflectance function was constructed using estimates from transmission, electron-energy-loss, etc., data above 11.8 eV, and direct measurements of reflectance at lower energies. This was then analyzed and the resulting optical functions compared with the input. The trial function was successively modified--primarily by the substitution of experimental data where available--until the calculated and measured optical functions agreed.

Throughout, the results were checked against a number of optical sum rules to ensure agreement with independent theoretical and experimental constraints (see Ref. 7 and citations therein). This disclosed that the reported oscillator strength in the L-absorption region was consistently too high by ~14 ½ %. The absorption coefficient in this region has generally been measured in transmission using thin films that exhibit a surface component of absorption.[78,79] To compensate for this, an ad hoc reduction was made in the data based on the thin-film measurements of Lukirskii et al.,[105] Fomichev and Lukirskii,[91,92] Haensel et al.,[89] and Gähwiller and Brown.[90] This reduction brought the calculated absorption coefficient into agreement with both the f sum rule and with later measurements by Balzarotti et al.,[79] who separated surface and bulk absorption. While the latter data extend only 10 eV above the L edge, the bulk $k(\omega)$ values of Balzarotti et al. are consistently some 15% below the thin-film $k(\omega)$ values used by Shiles et al.[7] in preparing their original input in this range. This is in agreement with the contention that previous thin-film measurements were systematically too large.

While this correction is very important in the soft x-ray region of the spectrum, it had negligible effect on the optical constants below the plasma frequency as determined by the Kramers-Kronig analysis.

The results of the analysis for the refractive index and the reflectance between the infrared and the $L_{II,III}$ edge are given in Appendix A. Given for comparison are the in situ uhv ellipsometric measurements of Mathewson and Myers,[87] the uhv reflectance data of Bennett et al.,[25] and the vacuum ultraviolet transmission and reflectance-angular-variation measurements of Ditchburn and Freeman.[50] The index results are graphed in Figure 4. It will be seen that the Kramers-Kronig analysis is in good agreement with direct measurements made by Mathewson and Myers[87] in the visible and the IR. The

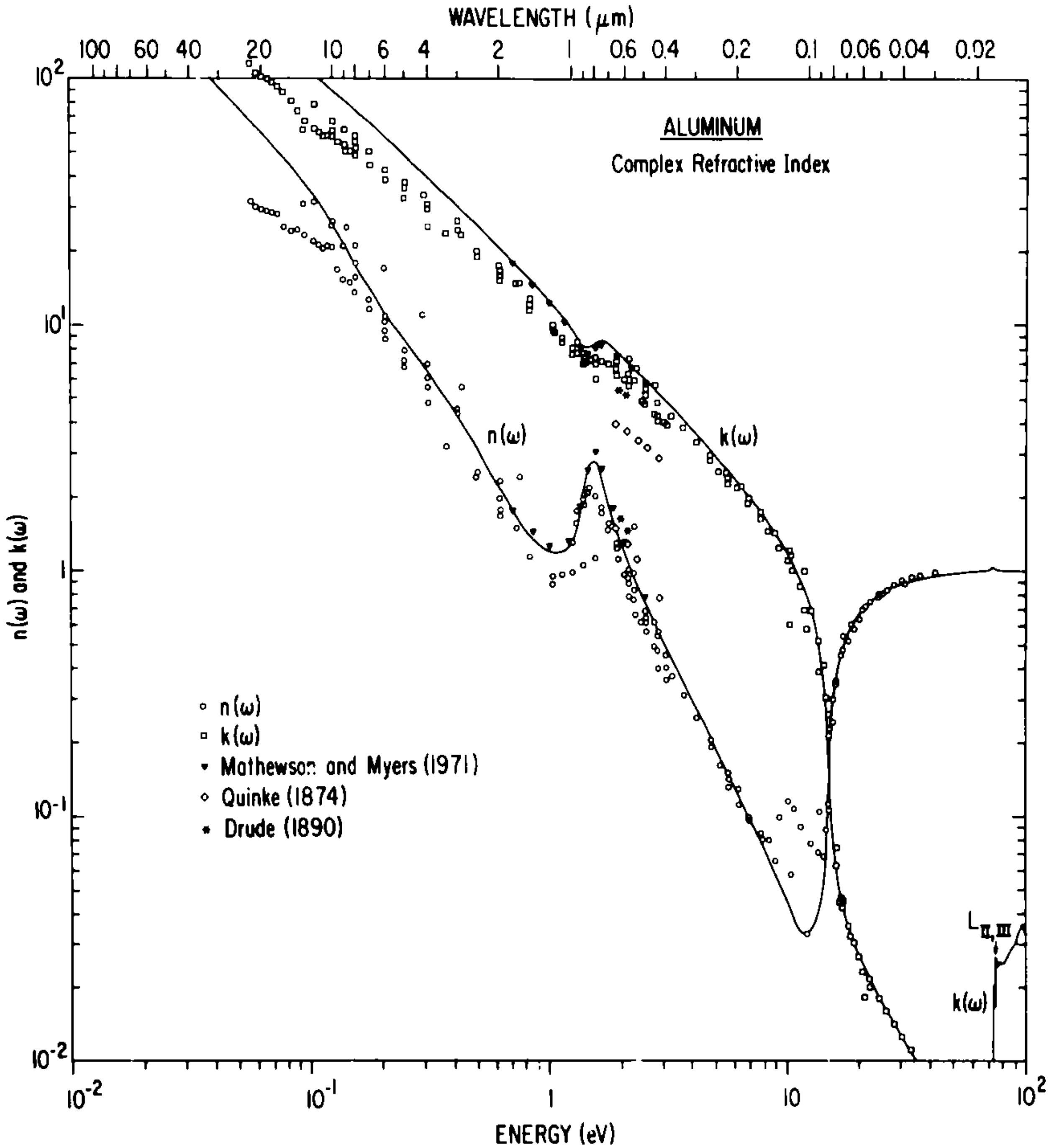

Fig. 4. The Complex Refractive Index [n(ω) + ik(ω)] of Metallic Aluminum. The solid curve is taken from Shiles et al.'s analysis of uhv reflectance data (Ref. 7). A portion of the uhv ellipsometric data of Matthewson and Myers (Ref. 87) is given for comparison. Quincke's (Ref. 28) and Drude's (Ref. 29) results for polished bulk samples are shown for historical interest; considering the materials and techniques available, these early measurements are remarkedly good, especially for n(ω). The remainder of the data points are given to show the range of values of n(ω) and k(ω) reported in the literature. Most refer to evaporated films prepared in conventional or high vacuum and measured using polarimetric, interferometric, etc., methods. The sources of these data are Refs. 9, 10, 22, 23, 24, 46, 50, 52, 62, 63, 70, 72, 83, and 108-116. Note that the n(ω) curve and the k(ω) curve cross each other at roughly 15 eV, the conduction electron plasmon energy. This corresponds to the condition $\epsilon_1(\omega_p) = n^2(\omega_p) - k^2(\omega_p) = 0$. The onset of the L absorption appears in the lower right corner. The corresponding dispersion is visible as a little "pimple" on the index curve near 72 eV.

difference between the Kramers-Kronig analysis and the measurements--less than 11% in $n(\omega)$ and 8% or less in $k(\omega)$--gives an indication of the uncertainty of the data.

A large number of optical constant measurements have been reported[9,10,22,23,24,46,50,52,62,63,70,72,83,106-116] for films prepared on normal substrates in high vacuum and subsequently exposed to air. The resulting "effective" optical constants describe contaminated aluminum surfaces made with no special attempt to produce ultra-smooth films. A number of these measurements are compared with values derived from uhv films in Fig. 4. Over most of the spectrum the effective optical constants for the oxidized surface lie below those for the uhv films. This is most pronounced in the IR, where effective optical constants 25% or more smaller than the uhv values are common. In the visible the effective constants are generally 10 to 15% lower than the uhv values, while in the UV the effective constants are surprisingly close to the uhv values. The exception is for the effective $n(\omega)$ near the surface plasmon frequency, ω_s. Here there is a "bump" in the effective index presumably arising from dispersion associated with the apparent "absorption" of the surface plasmon and light scattering by films with rough surfaces.

B. Room-Temperature Dielectric Function and Normal Reflectance

The dielectric function covering the complete energy range involved in the Kramers-Kronig analysis is given in Fig. 5 and in abridged form in Appendix B. This set of data includes the 14.5% reduction in the high-energy side of the $L_{II,III}$ edge needed to obtain agreement with the f sum rule and recent transmission measurements[79] taking surface effects into account. The energy intervals used in the table have been chosen to give closely spaced points in regions of pronounced structure, such as interband absorption and x-ray edges. Intermediate points can be found by interpolation, noting that the dielectric function generally has a power-law dependence on energy in regions removed from interband edges. Near the edges the energy spacing is too coarse to show all the x-ray fine structure. For details of this spectral region, see Refs. 117 and 118.

The $\varepsilon_2(\omega)$ curve in Fig. 5 discloses unexpected discontinuities in slope: a small discontinuity near 7 eV and a larger discontinuity near 15 eV. These are not readily apparent in the other optical functions, specifically in $n(\omega)$ and $k(\omega)$. These features may be extraneous, arising from the joining of data from different sources. This is mostly probably the case for the discontinuity near 7 eV, where additional uncertainty was introduced from reading published graphical data.

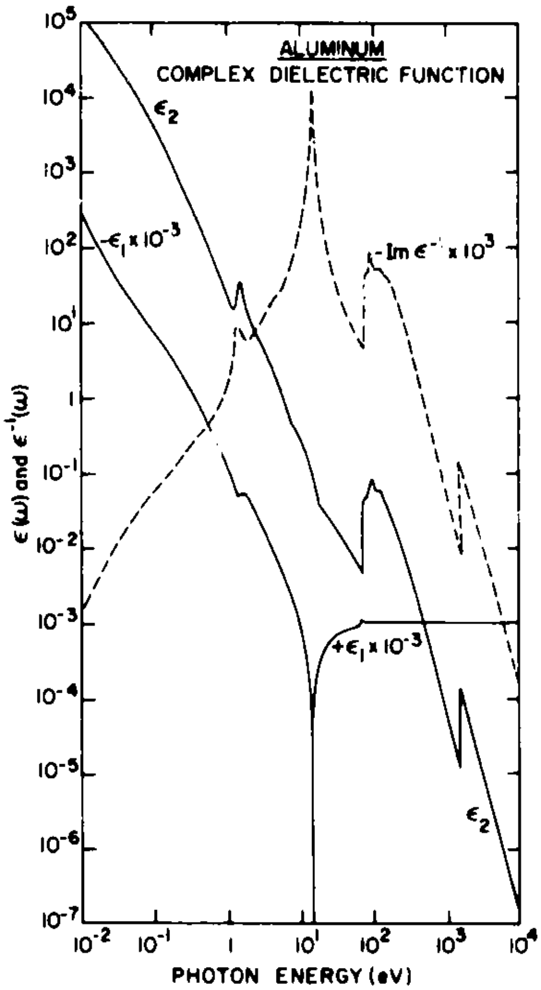

Fig. 5. The Complex Dielectric Response Function of Metallic Aluminum, after Shiles et al. (Ref. 7). The real part, $\varepsilon_1(\omega)$, is negative with large absolute values at low energies, vanishes at $\hbar\omega_p$ = 15.0 eV (the plasma energy for conduction electrons), and is positive and approaches unity at higher energies. The imaginary part, $\varepsilon_2(\omega)$, is also largest at low energies and decreases with energy, except at thresholds for newer modes of excitation (first at the beginning of the 1.5 eV interband excitation of valence electrons, next at the L-shell threshold, and finally at the K-shell threshold). The quantity $\mathrm{Im}[-1/\varepsilon(\omega)]$, which governs the energy transfer from fast charged particles, shows a prominent maximum near $\hbar\omega_p$ and is small at both lower and higher energies.

However, the situation is not so clear for the larger discontinuity near 15 eV (the plasma frequency). Here the ε_2 data fall off significantly faster below 15 eV than between 15 eV and the $L_{II,III}$ edge. This is contrary to the simple expectation, based on single-particle excitations, that at photon energies high compared to the principal interband transition energies, the valence-electrons should behave as almost free electrons so that their contribution to ε_2 should be approximately Drude-like; i.e., $\varepsilon_2(\omega) \sim \omega^{-3}$. A possible explanation is that the change in slope is an experimental artifact: below 15 eV, the $\varepsilon_2(\omega)$ data are based primarily on samples prepared in uhv, whereas from 15 eV to the $L_{II,III}$ edge, the samples were prepared in conventional vacua and measurements were made in air. Over the latter range, surface contamination could lead to significant errors in the optical constants reported by Ditchburn and Freeman.[50] Such an error cannot be detected as a violation of the f sum rule to within the accuracy of present data, since the contribution to the f sum rule over the region in question is of the order of a few tenths of an electron per atom.

A second and more intriguing possibility is that there is a deviation of the optical properties from their random-phase-approximation values above the plasma frequency. Just such an effect has been proposed by Hopfield[119] as a result of the dynamic screening of the phonon--or disorder--contribution to the optical absorption. A third possibility[120] is the excitation of bulk plasmons by oscillating changes induced at the metal surface by the exciting light; however, studies [121] of the surface photoelectric effect suggest the latter process is negligible. New measurements on well-characterized uhv samples in this energy range are needed to clarify this situation. Such experiments should be possible with the increasing availability of synchrotron radiation sources.

The dielectric function and optical properties for aluminum at room temperature recommended by Shiles et al.[7] are given in Appendix C for the original 506-point mesh used in their self-consistent Kramers-Kronig analysis. This tabulation covers the energy range of 0.04 eV to 10 keV and is available in the form of punched cards from the authors or on magnetic tape from:

National Energy Software Center
Argonne National Laboratory
9700 South Cass Avenue
Argonne, Illinois 60439.

In addition, the tables include values of the reflectance (the square of the amplitude reflection coefficient)

$$R(\omega) = \left| \frac{n(\omega) - 1 + i\,k(\omega)}{n(\omega) + 1 + i\,k(\omega)} \right|^2 , \tag{7}$$

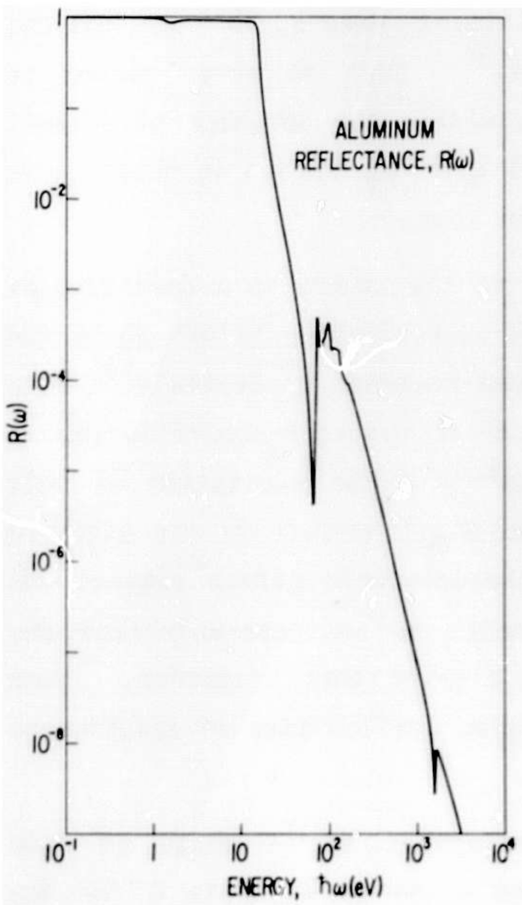

Fig. 6. The Reflectance of Metallic Aluminum. These values were calculated for normal incidence on a smooth, clean aluminum surface in vacuum from the n and k values of Shiles et al. (Ref. 7) via Eq. 7.

and the phase shift of the magnetic field vector

$$\theta = \tan^{-1} \frac{2k}{n^2 + k^2 - 1} \tag{8}$$

for reflectance at normal incidence from a smooth, clean aluminum surface in vacuum. Note that the phase shifts of the magnetic and electric fields differ by π, so that for a perfect conductor $\theta(0) = 0$. $R(\omega)$ and $\theta(\omega)$ are given graphically in Figs. 6 and 7.

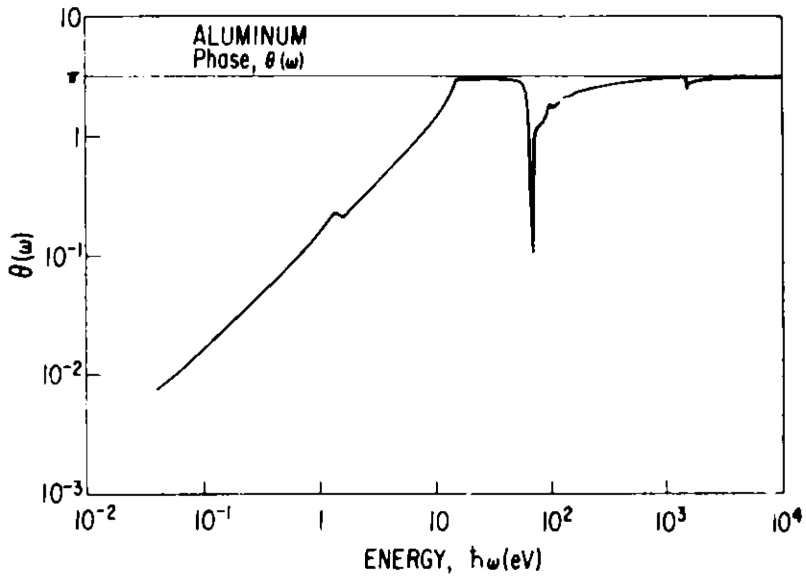

Fig. 7. The Phase of the Reflectivity of Metallic Aluminum. These values were calculated for normal incidence on a smooth, clean aluminum surface in vacuum from the n and k values of Shiles et al. (Ref. 7) via Eq. 8.

C. Temperature Dependence

The effect of temperature on the optical properties of aluminum has been studied directly with ellipsometry by Liljenvall et al.[88] and by Mathewson and Myers,[5] who found $\sigma(\omega)$ as a function of energy and temperature as shown in Fig. 8. As the temperature rises, the 1.5-eV interband transition shows a pronounced broadening, shifts toward lower energies, and becomes weaker. The free-electron contribution also shows a broadening, but becomes stronger with rising temperature. This is in line with the fact that interband transitions are not observed in the liquid metal,[84] as all the conduction-electron oscillator strength has been transferred to the Drude-like intraband term. The ellipsometric results have been analyzed[5] within the framework of the Ashcroft-Sturm[15] two-band model for the temperature dependence of the Drude parameters, the Fourier components of the crystal field, and the interband relaxation time (see Table I and Ref. 5).

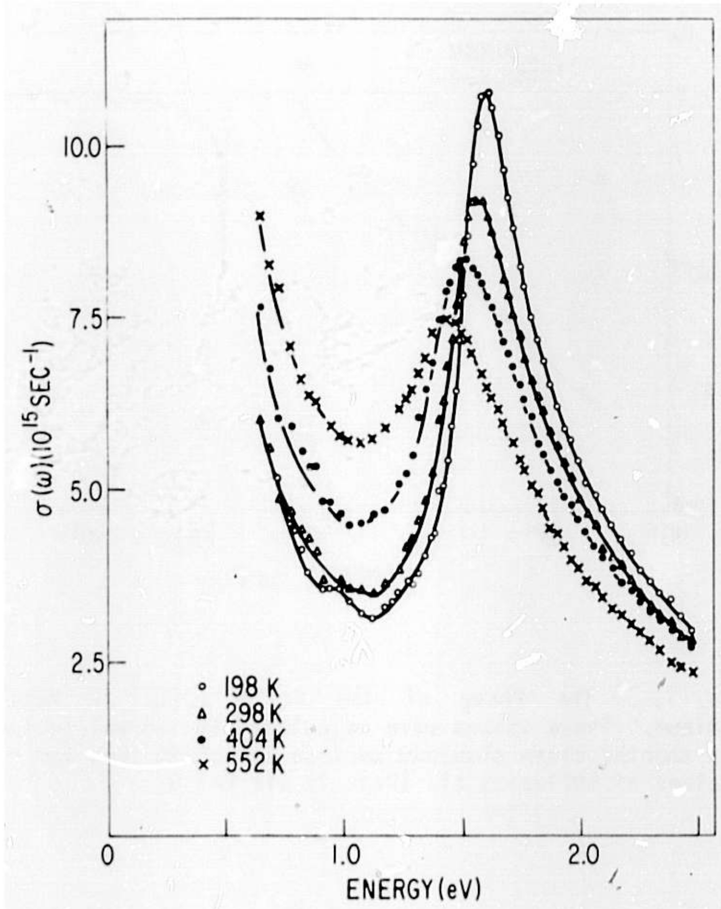

Fig. 8. The Optical Conductivity (real part) of Clean Polycrystalline Aluminum Films. The films were deposited at room temperature, after Mathewson and Myers (Ref. 5).

As a result of the high values of n(ω) and k(ω) in the visible and infrared, even a large variation of the optical constants with temperature produces only a small change in the reflectance, R. This effect has been recently investigated in thermomodulation studies of Rosei and Lynch.[122] The results are rather featureless, except near the "1.5-eV" interband absorption. They show that dR/dT is negative below about 1.3 eV (0.95 μm) and positive at higher energy. This is consistent with a broadening and shift toward low energies of the interband transition with rising temperature. Although the temperature modulation involved was not determined, the thermomodulation results may be scaled approximately using Pudkov's measurements[123] of reflectance as a function of temperature at 1.96 eV (0.633 μm). Pudkov reports a value for dR/dT of about 4×10^{-5} $(°C)^{-1}$ at this wavelength.

APPENDIX A

Optical Constants of Aluminum 0.039-75 eV

In this appendix we tabulate the optical constants of evaporated metallic aluminum films at room temperature from 32 μm to the $L_{II,III}$ edge. Columns labeled "SSIS" are the composite values given by Shiles et al.[7]; over the energies given here these data are based primarily on the Kramers-Kronig analysis of reflectance measurements of uhv films from 32 to 0.1 μm, as explained in the text. These results are shown graphically in Figs. 2 and 4. The uhv reflectance data of Bennett et al.[25] are given in columns labeled "BSA". The in situ uhv ellipsometric data of Mathewson and Myers[87] are given in columns labeled M & M, and the vacuum-uv transmission and angular-dependence-of-reflection measurements of Ditchburn and Freeman[50] are given in columns labeled D & F.

The reflectance values given in the column labeled $\bar{R}_{hv}$ are an average for representative films which have been prepared in conventional high vacuum ($\sim10^{-5}$ - 10^{-6} Torr) and subsequently exposed to the atmosphere. These data are given graphically as the "high-vacuum" curve in Fig. 2. The properties of such oxidized films are, of course, not unique; however, films prepared by rapid evaporation in high vacuum and exposed to clean dry air in a normal laboratory environment generally are reported to have reflectances approximately 1% lower than the values for unoxidized films prepared in UHV over the infrared and visible. At these wavelengths the reflectance tabulated is essentially the same as that for the NBS reference standard first-surface aluminum mirror[56] and high-quality commercial mirrors.[57] In the ultraviolet, such films generally show a sharp fall off of reflectance. This is a result of both absorption by surface oxides which become appreciable above 6.8 eV (see Sections II B1 and II B2), and scattering and surface-plasmon absorption resulting from surface roughness (see Section II B3). In general the reflectance shows great variability in the ultraviolet, unless care is exercised to control surface roughness. The data given here for oxidized films prepared in high vacuum are based on measurements of Beattie,[10] Strong,[21] Hass,[43,52] Sabine,[53] Banning,[54] Walker et al.,[55] Weidner and Hsia,[56] and Major.[57] In preparing the tabulation of reflectance values for oxidized films, an extrapolation of the available data to energies below 0.1 eV has been made on the assumption that there is no dramatic increase in oxide absorption in this energy range. This is based on the fact that the oxide thickness is small relative to the wavelength so that the films lies at a node in the electric vector of the total radiation field.[43]

Table II. Optical Constants of Aluminum

Energy		λ	Refractive Index, n			Extinction Coefficient, k			Reflectance				
eV	cm^{-1}	µm	SSIS	M&M	D&F	SSIS	M&M	D&F	SSIS	BSA	M&M	D&F	$\overline{R}_{hv}$
.038745	312.5	32	103			208			.992	.9933			.985
.04	322.62	31	98.6			204			.992				.985
.041328	333.33	30	94.2			199			.992	.9928			.985
.04428	357.14	28	86.3			189			.992	.9923			.985
.045	362.95	27.55	84.7			186			.992				.985
.047687	384.62	26	79.1			178			.992	.9918			.985
.05	403.27	24.8	75			172			.992				.984
.05166	416.66	24	72.2			168			.991	.9912			.984
.055	443.6	22.54	68.3			160			.991				.984
.056357	454.55	22	66.9			157			.991	.9907			.984
.06	483.93	20.66	62.9			151			.991				.984
.061992	499.99	20	60.7			147			.99	.9902			.984
.065	524.26	19.07	57.6			143			.99				.984
.068881	555.56	18	54.7			137			.99	.9896			.983
.07	564.58	17.71	53.8			136			.99				.983
.075	604.91	16.53	49.7			129			.99				.983
.077491	625	16	47.7			127			.99	.9892			.983
.08	645.24	15.5	46			124			.99				.983
.085	685.56	14.59	42.8			119			.989				.983
.088561	714.29	14	40.5			116			.989	.9886			.983
.09	725.89	13.78	39.7			114			.989				.983
.095	766.22	13.05	36.8			110			.989				.982
.095373	769.23	13	36.6			109			.989	.9884			.982
.1	806.55	12.4	34.5			106			.989				.982
.10332	833.32	12	33			103			.989	.9882			.982
.11	887.2	11.27	30.2			98.4			.989				.982
.11271	909.06	11	29.2			96.6			.989	.9879			.982
.12	967.86	10.33	26.6			92.2			.989				.981
.12398	999.96	10	25.3			89.8			.988	.9876			.981
.13	1048.5	9.537	23.5			86.5			.988				.981
.13776	1111.1	9	21.5			82.6			.988	.9874			.98
.14	1129.2	8.856	20.9			81.5			.988				.98
.15	1209.8	8.266	18.6			77			.988				.98
.15498	1250	8	17.5			74.9			.988	.9872			.98
.16	1290.5	7.749	16.5			72.7			.988				.98
.17	1371.1	7.293	14.9			68.8			.988				.979
.17712	1428.6	7	14			66.2			.988	.9866			.979
.18	1451.8	6.888	13.7			65.2			.988				.979
.19	1532.4	6.526	12.7			62.2			.987				.978
.2	1613.1	6.199	11.7			59.4			.987				.978
.20664	1666.6	6	11.1			57.6			.987	.9856			.978

Table II (continued). Optical Constants of Aluminum

Energy		λ	Refractive Index, n			Extinction Coefficient, k			Reflectance				
eV	cm^{-1}	µm	SSIS	M&M	D&F	SSIS	M&M	D&F	SSIS	BSA	M&M	D&F	$\overline{R}_{hv}$
.225	1814.7	5.51	9.85			53.2			.987				.977
.24797	2000	5	8.67			48.6			.986	.9843			.977
.25	2016.4	4.959	8.59			48.2			.986				.977
.275	2218	4.509	7.61			44.3			.985				.976
.3	2419.6	4.133	6.76			41			.984				.976
.30996	2500	4	6.43			39.8			.984	.9826			.975
.325	2621.3	3.815	6			38.1			.984				.975
.35	2822.9	3.542	5.44			35.6			.983				.975
.375	3024.5	3.306	4.88			33.4			.983				.974
.4	3226.2	3.1	4.45			31.5			.983				.974
.41328	3333.3	3	4.24			30.6			.982	.9805			.973
.45	3629.5	2.755	3.68			28.3			.982				.973
.5	4032.7	2.48	3.07			25.6			.982				.972
.55	4436	2.254	2.62			23.3			.981				.971
.6	4839.3	2.066	2.27			21.4			.981				.97
.61992	4999.9	2	2.15			20.7			.98	.9779			.97
.65	5242.6	1.907	1.99			19.8			.98				.97
.7	5645.8	1.771	1.77	1.7549		18.3	17.75		.979		.97825		.969
.75	6049.1	1.653	1.59	1.59		17.1	16.478		.979		.97714		.968
.8	6452.4	1.55	1.44	1.5		16	15.5		.978		.97566		.967
.82657	6666.7	1.5	1.38			15.4			.977	.9742			.967
.85	6855.6	1.459	1.33	1.4284		14.9	14.527		.977		.97366		.966
.9	7258.9	1.378	1.26	1.3463		14	13.704		.975		.97214		.964
.95	7662.2	1.305	1.23	1.2974		13.2	12.911		.973		.96982		.963
1	8065.5	1.24	1.21	1.2512		12.5	12.189		.97		.96742		.96
1.0332	8333.2	1.2	1.21			12			.968	.9637			.958
1.05	8468.7	1.181	1.21	1.2247		11.8	11.554		.967		.96462		.957
1.1	8872	1.127	1.2	1.2264		11.2	10.886		.963		.96027		.953
1.15	9275.3	1.078	1.21	1.2497		10.6	10.323		.958		.95522		.948
1.2	9678.6	1.033	1.26	1.3151		10	9.7329		.952		.94744		.942
1.2398	10000	1	1.35			9.58			.944	.9402			.934
1.25	10082	.9919	1.37	1.4142		9.49	9.1924		.943		.93737		.932
1.3	10485	.9537	1.47	1.5768		8.95	8.6883		.932		.9232		.918
1.3051	10526	.95	1.49			8.88			.93	.9243			.916
1.3404	10811	.925	1.77			8.49			.911	.9075			.902
1.35	10888	.9184	1.86	1.8176		8.44	8.1427		.906		.90207		.897
1.3776	11111	.9	2.06			8.3			.895	.8908			.884
1.4	11292	.8856	2.24	2.1355		8.21	7.7499		.885		.87778		.874
1.417	11429	.875	2.38			8.18			.878	.8744			.868
1.45	11695	.8551	2.58	2.5298		8.21	7.6092		.872		.85618		.86
1.4586	11765	.85	2.61			8.22			.87	.8677			.859

Table II (continued). Optical Constants of Aluminum

Energy		λ	Refractive Index, n			Extinction Coefficient, k			Reflectance				
eV	cm^{-1}	μm	SSIS	M&M	D&F	SSIS	M&M	D&F	SSIS	BSA	M&M	D&F	$\bar{R}_{hv}$
1.5	12098	.8266	2.74	2.94		8.31	7.7552		.868		.84458		.858
1.5028	12121	.825	2.75			8.31			.868	.8657			.858
1.5498	12500	.8	2.8			8.45			.869	.8676			.86
1.55	12501	.7999	2.8	3.0395		8.45	8.077		.87		.85093		.86
1.5998	12903	.775	2.63			8.6			.879	.8773			.868
1.6	12905	.7749	2.62	2.8732		8.6	8.2313		.879		.86113		.868
1.65	13308	.7514	2.41	2.5745		8.62	8.254		.888		.87271		.876
1.6531	13333	.75	2.4			8.62			.888	.8862			.876
1.7	13711	.7293	2.14	2.3368		8.57	8.1523		.897		.87954		.882
1.75	14115	.7085	1.91	2.1306		8.39	8.0025		.903		.88458		.883
1.7712	14286	.7	1.83			8.31			.905	.8977			.89
1.8	14518	.6888	1.74	1.9419		8.21	7.8276		.907		.88892		.893
1.85	14921	.6702	1.6	1.7758		8.01	7.6586		.91		.89296		.896
1.9	15324	.6526	1.49	1.6281		7.82	7.4934		.912		.89672		.899
1.9075	15385	.65	1.47			7.79			.912	.9057			.899
1.95	15728	.6358	1.39	1.5068		7.65	7.3668		.913		.90047		.901
2	16131	.6199	1.3	1.4011		7.48	7.2085		.915		.90292		.903
2.05	16534	.6048	1.22	1.3055		7.31	7.0855		.916		.90594		.904
2.0664	16666	.6	1.2			7.26			.917	.9117			.904
2.1	16937	.5904	1.15	1.2198		7.15	6.9273		.918		.90779		.905
2.15	17341	.5767	1.08	1.145		7	6.7684		.919		.90915		.906
2.2	17744	.5636	1.02	1.0686		6.85	6.6439		.92		.91172		.907
2.25	18147	.551	.963	1.0046		6.7	6.5199		.921		.91363		.908
2.2543	18182	.55	.958			6.69			.921	.9157			.908
2.3	18551	.5391	.912	.94408		6.55	6.3554		.922		.91451		.909
2.35	18954	.5276	.867	.89107		6.42	6.2285		.922		.91538		.909
2.4	19357	.5166	.826	.85227		6.28	6.1013		.923		.91615		.91
2.45	19760	.5061	.789	.81783		6.15	5.9303		.923		.91497		.911
2.4797	20000	.5	.769			6.03			.923	.9162			.911
2.5	20164	.4959	.755	.77909		6.03	5.8401		.923		.91639		.911
2.6	20970	.4769	.695			5.8			.924				.912
2.7	21777	.4592	.644			5.58			.924				.913
2.7552	22222	.45	.618			5.47			.924	.9175			.913
2.8	22583	.4428	.598			5.38			.924				.913
2.9	23390	.4275	.558			5.2			.924				.914
3	24196	.4133	.523			5.02			.924				.914
3.0996	25000	.4	.49			4.86			.924	.9194			.915
3.1	25003	.4	.49			4.86			.924				.915
3.2	25809	.3875	.46			4.71			.924				.915
3.3	26616	.3757	.432			4.56			.924				.915
3.4	27423	.3647	.407			4.43			.924				.914

Table II (continued). Optical Constants of Aluminum

Energy		λ	Refractive Index, n			Extinction Coefficient, k			Reflectance				
eV	cm^{-1}	μm	SSIS	M&M	D&F	SSIS	M&M	D&F	SSIS	BSA	M&M	D&F	$\bar{R}_{hv}$
3.5	28229	.3542	.385			4.3			.925				.914
3.5424	28571	.35	.375			4.24			.925	.9205			.914
3.6	29036	.3444	.364			4.17			.925				.913
3.7	29842	.3351	.344			4.06			.925				.913
3.8	30649	.3263	.326			3.95			.925				.912
3.9	31455	.3179	.31			3.84			.925				.911
4	32262	.31	.294			3.74			.925				.91
4.1328	33333	.3	.276			3.61			.925	.9208			.909
4.25	34278	.2917	.261			3.51			.925				.908
4.5	36295	.2755	.233			3.3			.925				.905
4.75	38311	.261	.209			3.11			.925				.901
5	40327	.248	.19			2.94			.924				.894
5.25	42344	.2362	.172			2.79			.925				.884
5.5	44360	.2254	.155			2.64			.926				.873
5.75	46376	.2156	.141			2.51			.926				.858
6	48393	.2066	.13			2.39			.926				.841
6.25	50409	.1984	.119			2.28			.926				.82
6.5	52426	.1907	.11			2.17			.926				.793
6.75	54442	.1837	.102			2.07			.926				.766
7	56458	.1771	.0946			1.98			.926				.735
7.25	58475	.171	.088			1.9			.926				.698
7.5	60491	.1653	.082			1.81			.927				.656
7.75	62507	.16	.0765			1.74			.927				.616
8	64524	.155	.0716			1.66			.927				.579
8.25	66540	.1503	.0671			1.59			.927				.543
8.5	68556	.1459	.063			1.53			.927				.51
8.75	70573	.1417	.0592			1.46			.927				.478
9	72589	.1378	.0557			1.4			.928				.448
9.5	76622	.1305	.0495			1.29			.928				.388
10	80655	.124	.0442			1.18			.929				.328
10.5	84687	.1181	.0396			1.08			.929				.27
11	88720	.1127	.0356			.978			.93				.215
11.5	92753	.1078	.0331			.883			.928				.165
12	96786	.1033	.0328		.033	.791		.58	.922			.906	.127
12.5	100818	.09919	.0344			.7			.912				.102
13	104851	.09537	.0376			.609			.856				.086
13.5	108884	.09184	.0409		.104	517		.39	.879			.697	.074
14	112917	.08856	.0481			.416			.849				.064
14.5	116949	.08551	.0616			.301			.798				.057
15	120982	.08266	.125		.225	.153		.22	.612			.419	.05
15.5	125015	.07999	.258			.0777			.35				

Table II (continued). Optical Constants of Aluminum

Energy		λ	Refractive Index, n			Extinction Coefficient, k			Reflectance				
eV	cm^{-1}	µm	SSIS	M&M	D&F	SSIS	M&M	D&F	SSIS	BSA	M&M	D&F	$\overline{R}_{hv}$
16	129047	.07749	.351		.345	.0595		.0632	.233			.239	
16.5	133080	.07514	.419			.0487			.168				
17	137113	.07293	.474		.445	.0423		.0424	.128			.148	
17.5	141146	.07085	.52			.0381			.1				
18	145178	.06858	.558		.52	.0348		.0355	.0309			.1	
18.5	149211	.06702	.591			.0324			.0664				
19	153244	.06526	.62		.58	.0302		.0307	.0554			.071	
19.5	157277	.06358	.646			.0284			.0467				
20	161309	.06199	.668		.635	.0268		.0267	.0398			.0501	
21	169375	.05904	.707			.0242			.0296				
22	177440	.05636	.74		.718	.0222		.0213	.0226			.0271	
23	185506	.05391	.766			.0205			.0177				
24	193571	.05166	.789		.785	.019		.0182	.014			.0146	
25	201637	.04959	.809			.0177			.0113				
26	209702	.04769	.826		.838	.0165		.0159	.0092			.00784	
27	217768	.04592	.841			.0155			.00758				
28	225833	.04428	.854		.88	.0145		0141	.0063			.00413	
29	233898	.04275	.865			.0135			.00528				
30	241964	.04133	.876		.912	.0125		.0125	.00444			.00216	
31	250029	.04	.885			.0116			.00375				
32	258095	.03875	.894			.0111			.00317				
33	266160	.03757	.902		.943	.0107		.011	.00271			8.93E-4	
34	274226	.03647	.909			.0102			.00233				
36	290357	.03444	.921		.96	.00932		.0095	.00173			4.4E-4	
38	306488	.03263	.931			.00871			.0013				
40	322619	.031	.94			.00816			9.89E-4				
45	362946	.02755	.957			.00682			5.01E-4				
50	403273	.0248	.969			.00587			2.57E-4				
55	443601	.02254	.979			.00508			1.21E-4				
60	483928	.02066	.987			.00441			4.64E-5				
65	524255	.01907	.995			.00417			9.25E-6				
70	564583	.01771	1.01			.00352			1.27E-5				
71	572648	.01746	1.01			.00346			2.75E-5				
72	580713	.01722	1.02			.00346			6.85E-5				
73	588779	.01698	1.02			.0191			2.33E-4				
74	596844	.01675	1.01			.0242			1.97E-4				
75	604910	.01653	1.01			.024			1.74E-4				

APPENDIX B

Dielectric Function of Aluminum (short tabulation)

In this appendix we tabulate the dielectric function for clean, smooth evaporated aluminum films at room temperature as interpolated on an energy mesh from the results of Shiles et al. (Ref. 7). As explained in detail in the text, these data are based primarily on the analysis of reflectance measurements below the $L_{II,II}$ edge and on transmission measurements above the edge. They are in close agreement with direct ellipsometric measurements on oxide-free films by Mathewson and Myers[87] in the range 0.7 to 2.5 eV.

Extrapolation of the tabular data may be made as follows:

1) Low-energy extrapolations. The Drude Model, Eq. 1, with $\hbar\Omega_p$ = 11.5 eV and $\hbar\gamma$ = 50.6 meV [$\sigma(0) = 3.16 \times 10^{17}$ sec^{-1}] fits on continuously at 0.04 eV, but with a small discontinuity in slope. However, it should be recognized that, while the dc conductivity is in excellent agreement with the measured value ($3.18\text{-}3.28 \times 10^{17}$ sec^{-1}),[124-125] Ω_p and γ are somewhat outside the range recommended by Smith and Segall[14] (see Table I). This represents a negligible conflict since for the high reflectances (>99%) beyond 20 μm the experimental error (± 0.1%) in the reflectance measurements used to obtain the dielectric function translates into an uncertainty of the order of ±25% in $\varepsilon(\omega)$ even in favorable cases. The values of Smith and Segall arise from fits over the range 0.04-3 eV, not just at the lowest energy point, which is subject to considerable uncertainty.
2) High-energy extrapolations. $\varepsilon_1(\omega)$: At frequencies well above the K edge the real part of the dielectric function approaches $\varepsilon_1 \approx 1 - \omega_{p,t}^2/\omega^2$, where $\omega_{p,t}$ is the plasma frequency for the <u>total</u> electron density (13 electrons/atom). For aluminum at room temperature $\hbar\omega_{p,t} \approx$ 32.86 eV and the asymptotic form holds for photon energies beyond $\hbar\omega$ = 3000 eV. $\varepsilon_2(\omega)$: Beyond the K edge $\varepsilon_2(\omega)$ falls off very nearly as a power of energy, $\varepsilon_2(\omega) \sim \omega^{-\delta}$. The exponent varies slowly with energy; at 5000 eV, $\delta \sim 3.8$; at 10^4 eV, $\delta \sim 4.0$; and from 10^4 to 10^5 eV, it increases to δ = 4.2. An extrapolation from 10^4 eV using δ = 4.1 reproduces photoelectric data up to 10^5 eV reasonably well.

Table III. Dielectric Function of Aluminum

Energy,eV	ϵ_1	ϵ_2	Energy,eV	ϵ_1	ϵ_2	Energy,eV	ϵ_1	ϵ_2
.04	-31773	40168	.45	-785.73	208.33	2.1	-49.855	16.425
.045	-27581	31591	.5	-644.95	157.16	2.2	-45.829	13.944
.05	-24028	25829	.55	-536.6	122.17	2.3	-42.126	11.956
.055	-20840	21811	.6	-452.92	97.295	2.4	-38.792	10.381
.06	-18790	18956	.65	-386.35	78.532	2.5	-35.812	9.1113
.065	-16994	16416	.7	-332.78	64.879	2.6	-33.154	8.0664
.07	-15467	14577	.75	-289.02	54.332	2.7	-31.777	7.1883
.075	-14290	12858	.8	-252.48	46.07	2.8	-28.64	6.4398
.08	-13214	11380	.85	-221.46	39.819	2.9	-26.709	5.7995
.085	-12265	10160	.9	-194.99	35.454	3	-24.967	5.2581
.09	-11447	9048.6	.95	-172.78	32.454	3.2	-21.951	4.3266
.095	-10716	8080.2	1	-153.88	30.208	3.4	-19.424	3.6058
.1	-9963.6	7278.7	1.05	-137.69	28.45	3.6	-17.288	3.0346
.11	-8769.4	5939.9	1.1	-123.57	26.86	3.8	-15.463	2.5754
.12	-7787.2	4898.6	1.15	-110.51	25.665	4	-13.901	2.2027
.13	-6930.1	4065.1	1.2	-98.612	25.231	4.5	-10.833	1.5379
.14	-6204.7	3409.8	1.22	-93.974	25.474	5	-8.6168	1.1199
.15	-5577.9	2858.6	1.24	-89.971	25.923	5.5	-6.9646	.81915
.16	-5015.8	2407.2	1.26	-86.2	26.1	6	-5.7	.62085
.17	-4512.1	2053.8	1.28	-82.271	26.11	6.5	-4.7106	.47906
.18	-4065.1	1791	1.3	-77.922	26.278	7	-3.9229	.37529
.19	-3702.8	1577.7	1.32	-72.927	27.485	7.5	-3.2853	.2974
.2	-3387.1	1393.2	1.34	-69.012	30.031	8	-2.7618	.23806
.21	-3096	1230.9	1.36	-66.705	32.535	8.5	-2.3268	.19224
.22	-2845.3	1103.6	1.38	-64.446	34.505	9	-1.9617	.15604
.23	-2622.2	994.94	1.4	-62.425	36.736	9.5	-1.6513	.12726
.24	-2424.3	905.18	1.42	-61.074	39.283	10	-1.386	.10421
.25	-2252.9	828.26	1.44	-60.939	41.511	10.5	-1.1566	.08517
.26	-2098.3	760.63	1.46	-60.708	43.079	11	-.95619	.069713
.27	-1963.5	701.32	1.48	-60.965	44.564	11.5	-.77942	.058537
.28	-1840.9	647.03	1.5	-61.503	45.609	12	-.6241	.051904
.29	-1730.9	598.74	1.52	-62.052	46.326	12.5	-.48873	.048139
.3	-1632	553.71	1.54	-62.953	47.064	13	-.37007	.045233
.31	-1540	511.51	1.56	-64.303	47.378	13.5	-.26564	.042292
.32	-1453.9	473.79	1.58	-66.272	46.672	14	-.17115	.040106
.33	-1373.8	441.56	1.6	-67.029	45.129	14.2	-.13652	.03928
.34	-1302.3	413.6	1.65	-68.525	41.606	14.4	-.10332	.038018
.35	-1237.7	387.14	1.7	-68.91	36.742	14.6	-.070376	.036441
.36	-1177.6	361.78	1.75	-66.676	31.998	14.8	-.037265	.036129
.37	-1121.6	337.73	1.85	-61.654	25.715	15	-.0078247	.038338
.38	-1057.8	315.76	1.9	-58.961	23.279	15.2	.020186	.038548
.39	-1017.6	296.83	1.95	-56.522	21.251	15.4	.04769	.039414
.4	-971.47	280.45	2	-54.236	19.502	15.6	.073266	.040811

Table III (continued). Dielectric Function of Aluminum

Energy,eV	ε_1	ε_2	Energy,eV	ε_1	ε_2	Energy,eV	ε_1	ε_2
15.8	.096931	.041612	75.5	1.0205	.04841	1400	.99957	1.7796E-5
16	.11946	.041735	76	1.0197	.048178	1450	.99961	1.5597E-5
17	.22322	.04013	77	1.0175	.050823	1500	.99966	1.3558E-5
18	.3103	.038346	78	1.0139	.049371	1510	.99968	1.3238E-5
19	.38348	.037448	79	1.0133	.049331	1520	.99969	1.2878E-5
20	.44595	.035822	80	1.0134	.04928	1530	.99971	1.2598E-5
25	.65365	.023627	82	1.0137	.051293	1540	.99974	1.2298E-5
30	.76651	.02197	84	1.0131	.054019	1550	.99978	1.1999E-5
35	.83681	.017966	86	1.011	.056799	1555	.99983	5.9093E-5
40	.88269	.015332	88	1.01	.05823	1556	.99982	6.2094E-5
45	.91527	.013043	90	1.0098	.062184	1557	.99983	5.8603E-5
50	.9389	.011383	92	1.0068	.067059	1558	.99984	6.5831E-5
55	.95813	.0099416	94	.99978	.070656	1559	.99985	8.2294E-5
60	.97456	.0087087	96	.99149	.071495	1560	.99985	1.0003E-4
62	.98101	.0084568	98	.98315	.06559	1561	.99985	1.2198E-4
64	.98756	.0082042	100	.98036	.05927	1562	.99985	1.4371E-4
66	.99398	.0077765	105	.98603	.0485	1563	.99983	1.6362E-4
68	1.0021	.0073387	110	.98712	.050591	1564	.99981	1.7089E-4
70	1.0125	.0070858	115	.984	.049469	1565	.99979	1.686E-4
71	1.02	.0069815	120	.98136	.047692	1570	.99976	1.6222E-4
72	1.0329	.0070415	125	.978	.046345	1580	.99973	1.5697E-4
72.1	1.035	.0069485	130	.97458	.040695	1590	.99971	1.5197E-4
72.2	1.0374	.0069398	135	.97559	.035113	1600	.9997	1.4762E-4
72.3	1.0404	.0068713	140	.97719	.032247	1650	.99968	1.3093E-4
72.4	1.0444	.006789	145	.97819	.030553	1700	.99968	1.1536E-4
72.5	1.0498	.0072644	150	.97907	.029245	1800	.9997	9.4264E-5
72.6	1.0609	.0081393	160	.97848	.027176	1900	.99972	7.6913E-5
72.7	1.0628	.025492	170	.97763	.021736	2000	.99974	6.4056E-5
72.8	1.0609	.041175	180	.97973	.019128	2500	.99983	2.7182E-5
72.9	1.0511	.040888	190	.98095	.016795	3000	.99988	1.4199E-5
73	1.0489	.039105	200	.982	.014904	3500	.99991	8.0064E-6
73.1	1.0516	.039983	250	.98619	.0083246	4000	.99993	4.8998E-6
73.2	1.0504	.049549	300	.98978	.0046841	5000	.99996	2.08E-6
73.3	1.0431	.053085	400	.99378	.0019393	6000	.99997	1.046E-6
73.4	1.0376	.051766	500	.9959	8.6947E-4	7000	.99998	5.7999E-7
73.5	1.0349	.050481	600	.99717	4.408E-4	8000	.99998	3.4E-7
73.6	1.0333	.049756	700	.99796	2.363E-4	9000	.99999	2.16E-7
73.7	1.032	.049488	800	.99845	1.4621E-4	10000	.99999	1.42E-7
73.8	1.0308	.049276	900	.99879	9.3552E-5			
73.9	1.0298	.049153	1000	.99904	6.222E-5			
74	1.0289	.049041	1100	.99922	4.3115E-5			
74.5	1.0249	.049278	1200	.99936	3.119E-5			
75	1.0221	.048564	1300	.99947	2.3194E-5			

APPENDIX C

Dielectric Function and Optical Properties of Aluminum 0.04-10^4 eV (Long Tabulation)

In this appendix we tabulate the dielectric function and optical properties for aluminum at room temperature given by Shiles et al. (Ref. 7) on the original 506-point mesh used in their self-consistent Kramers-Kronig analysis. Values of the reflectance and phase shift (of the magnetic field vector) are given for normal incidence. All digits in the computer output have been retained, even though only the first two are believed to be significant over most of the range.

Table IV. Dielectric Function and Optical Properties of Aluminum

Energy	Dielectric Function		Refractive Index		Reflectivity		
eV	ϵ_1	ϵ_2	n	k	R	θ (degrees)	θ (radians)
.04	-31773	40168	98.596	203.7	.99233	.45577	.0079547
.042	-30076	36207	92.177	196.4	.9922	.47814	.0083451
.044	-28334	32981	86.975	189.6	.99204	.49931	.0087146
.046	-26813	30297	82.598	183.4	.99187	.51945	.0090662
.048	-25374	27897	78.538	177.6	.9917	.53968	.0094192
.05	-24028	25829	74.997	172.2	.99153	.55936	.0097626
.052	-22750	23943	71.686	167	.99136	.57941	.010113
.054	-21370	22441	69.348	161.8	.99109	.59832	.010443
.056	-20379	21223	67.246	157.8	.9909	.61457	.010726
.058	-19502	20079	65.15	154.1	.99073	.63086	.011011
.06	-18790	18956	62.852	150.8	.99063	.64742	.0113
.062	-17989	17856	60.652	147.2	.99047	.66549	.011615
.064	-17360	16900	58.599	144.2	.99037	.68203	.011904
.066	-16612	15962	56.683	140.8	.99021	.70035	.012223
.068	-15929	15245	55.316	137.8	.99002	.71617	.0125
.07	-15467	14577	53.79	135.5	.98993	.73056	.012751
.072	-14982	13839	52.027	133	.98985	.74724	.013042
.074	-14511	13178	50.452	130.6	.98976	.76348	.013325
.076	-14072	12542	48.877	128.3	.98968	.77995	.013613
.078	-13633	11934	47.358	126	.9896	.79688	.013908
.08	-13214	11380	45.961	123.8	.98951	.81349	.014198
.082	-12817	10868	44.651	121.7	.98943	.82987	.014484
.084	-12446	10386	43.383	119.7	.98935	.84616	.014768
.086	-12097	9939.3	42.187	117.8	.98925	.86218	.015048
.088	-11808	9493.8	40.886	116.1	.98926	.87809	.015325
.09	-11447	9048.6	39.651	114.1	.98919	.89607	.015639
.092	-11144	8677.3	38.6	112.4	.98913	.91193	.015916
.094	-10880	8280.2	37.366	110.8	.98913	.92861	.016207
.096	-10546	7891.4	36.233	108.9	.98906	.94739	.016535
.098	-10245	7571	35.312	107.2	.98897	.9643	.01683
.1	-9963.6	7278.7	34.464	105.6	.98889	.98068	.017116
.105	-9365.3	6574.7	32.229	102	.9888	1.0214	.017828
.11	-8769.4	5939.9	30.186	98.39	.98867	1.0645	.018578
.115	-8263	5399.4	28.352	95.22	.98858	1.1054	.019293
.12	-7787.2	4898.6	26.577	92.16	.98851	1.1479	.020035
.125	-7342.3	4456.2	24.965	89.25	.98844	1.1907	.020782
.13	-6930.1	4065.1	23.498	86.5	.98837	1.2337	.021532
.135	-6549.7	3719.3	22.162	83.91	.9883	1.2766	.02228
.14	-6204.7	3409.8	20.919	81.5	.98825	1.3191	.023022
.145	-5889.3	3121.5	19.699	79.23	.98825	1.3621	.023773
.15	-5577.9	2858.6	18.572	76.96	.98822	1.407	.024556
.155	-5297.1	2622.8	17.518	74.86	.98322	1.4512	.025328
.16	-5015.8	2407.2	16.549	72.73	.98817	1.4979	.026144

Table IV (continued). Dielectric Function and Optical Properties of Aluminum

Energy	Dielectric Function		Refractive Index		Reflectivity		
eV	ϵ_1	ϵ_2	n	k	R	θ (degrees)	θ (radians)
.165	-4757.6	2221.7	15.703	70.74	.98811	1.5437	.026943
.17	-4512.1	2053.8	14.924	68.81	.98803	1.5904	.027758
.175	-4275.9	1910.7	14.274	66.92	.98789	1.6375	.02858
.18	-4065.1	1791	13.73	65.22	.98771	1.6823	.029362
.185	-3875.4	1681.9	13.214	63.64	.98757	1.7261	.030126
.19	-3702.8	1577.7	12.691	62.16	.98747	1.7696	.030885
.195	-3535.5	1481.9	12.207	60.7	.98735	1.8143	.031666
.2	-3387.1	1393.2	11.733	59.37	.98727	1.8574	.032418
.21	-3096	1230.9	10.856	56.691	.98705	1.9497	.034028
.22	-2845.3	1103.6	10.162	54.301	.98677	2.0387	.035582
.23	-2622.2	994.94	9.5501	52.09	.98648	2.1281	.037142
.24	-2424.3	905.18	9.0409	50.06	.98613	2.2165	.038686
.25	-2252.9	828.26	8.5857	48.235	.9858	2.3025	.040185
.26	-2098.3	760.63	8.1734	46.531	.98546	2.3887	.04169
.27	-1963.5	701.32	7.7939	44.992	.98517	2.4724	.043152
.28	-1840.9	647.03	7.4296	43.544	.98489	2.5568	.044624
.29	-1730.9	598.74	7.0933	42.204	.98464	2.6401	.046079
.3	-1632	553.71	6.7592	40.96	.98444	2.723	.047526
.31	-1540	511.51	6.4314	39.766	.98428	2.8076	.049003
.32	-1453.9	473.79	6.134	38.62	.98409	2.8936	.050502
.33	-1373.8	441.56	5.883	37.529	.98384	2.9796	.052003
.34	-1302.3	413.6	5.6613	36.529	.98358	3.0628	.053455
.35	-1237.7	387.14	5.4376	35.599	.98338	3.1449	.054888
.36	-1177.6	361.78	5.2115	34.71	.98323	3.2278	.056337
.37	-1121.6	337.73	4.9872	33.86	.98313	3.3116	.057798
.38	-1067.8	315.76	4.7806	33.025	.98299	3.3977	.059301
.39	-1017.6	296.83	4.6048	32.23	.98279	3.4832	.060794
.4	-971.47	280.45	4.4537	31.485	.98255	3.5671	.062257
.42	-890.76	249.35	4.1378	30.131	.98228	3.7315	.065126
.44	-818.88	221.07	3.8286	28.871	.98213	3.8991	.068051
.46	-754.37	196.5	3.5477	27.694	.98198	4.0693	.071023
.48	-696.69	175.42	3.2974	26.6	.98183	4.2409	.074018
.5	-644.95	157.16	3.0718	25.581	.98169	4.4138	.077035
.52	-598.2	141.4	2.8709	24.626	.98152	4.5885	.080085
.54	-555.93	128.09	2.6987	23.732	.98129	4.7643	.083152
.56	-518.3	116.58	2.5445	22.908	.98106	4.9383	.08619
.58	-484.21	106.16	2.398	22.135	.98087	5.1136	.089249
.6	-452.92	97.295	2.2729	21.403	.98061	5.2907	.09234
.65	-386.35	78.532	1.9875	19.756	.98009	5.7376	.10014
.7	-332.78	64.879	1.7699	18.328	.97939	6.1887	.10801
.75	-289.02	54.332	1.591	17.075	.97866	6.6461	.116
.8	-252.48	46.07	1.4437	15.955	.97783	7.1149	.12418
.85	-221.46	39.819	1.3325	14.941	.97669	7.5982	.13261

Table IV (continued). Dielectric Function and Optical Properties of Aluminum

Energy	Dielectric Function		Refractive Index		Reflectivity		
eV	ϵ_1	ϵ_2	n	k	R	θ (degrees)	θ (radians)
.9	-194.99	35.454	1.2643	14.021	.97493	8.0938	.14126
.95	-172.78	32.454	1.2291	13.202	.97257	8.5896	.14992
1	-153.88	30.208	1.2118	12.464	.96975	9.0892	.15864
1.05	-137.69	28.45	1.2059	11.796	.9665	9.5922	.16742
1.1	-123.57	26.86	1.2012	11.181	.963	10.107	.17639
1.15	-110.51	25.665	1.2127	10.582	.9585	10.659	.18603
1.2	-98.612	25.231	1.2603	10.01	.95213	11.235	.19608
1.22	-93.974	25.474	1.3022	9.7811	.94841	11.475	.20028
1.24	-89.971	25.923	1.3528	9.5813	.94441	11.688	.20399
1.26	-86.2	26.1	1.3901	9.3879	.94075	11.904	.20777
1.28	-82.271	26.11	1.4219	9.1811	.93691	12.146	.212
1.3	-77.922	26.278	1.4683	8.9486	.93184	12.425	.21685
1.32	-72.927	27.485	1.5823	8.6851	.92291	12.723	.22206
1.34	-69.012	30.031	1.7679	8.4934	.91138	12.884	.22487
1.36	-66.705	32.[illegible]	1.938	8.3941	.90199	12.914	.2254
1.38	-64.446	34.505	2.0804	8.293	.89367	12.955	.2261
1.4	-62.425	36.736	2.2369	8.2115	.88515	12.948	.22598
1.42	-61.074	39.283	2.4024	8.1759	.87746	12.862	.22448
1.44	-60.939	41.511	2.5293	8.2059	.8732	12.715	.22192
1.46	-60.708	43.079	2.6203	8.2203	.87009	12.619	.22024
1.48	-60.965	44.564	2.6973	8.2608	.86828	12.501	.21819
1.5	-61.503	45.609	2.7446	8.3088	.86782	12.402	.21645
1.52	-62.052	46.386	2.7768	8.3524	.86781	12.322	.21506
1.54	-62.953	47.064	2.7971	8.4129	.86867	12.234	.21352
1.56	-64.308	47.378	2.79	8.4907	.87092	12.15	.21206
1.58	-66.272	46.672	2.7189	8.5828	.8757	12.102	.21122
1.6	-67.029	45.129	2.6245	8.5975	.87941	12.159	.21222
1.65	-68.525	41.606	2.4127	8.6224	.88777	12.289	.21448
1.7	-68.91	36.742	2.1428	8.5733	.8972	12.539	.21885
1.75	-66.676	31.998	1.9079	8.3855	.90312	12.946	.22595
1.8	-64.292	28.572	1.7411	8.2051	.90694	13.312	.23234
1.9	-58.961	23.279	1.4881	7.8215	.91164	14.075	.24566
2	-54.236	19.502	1.3038	7.479	.91485	14.795	.25821
2.1	-49.855	16.425	1.148	7.1535	.91768	15.528	.27102
2.2	-45.829	13.944	1.0184	6.8459	.92003	16.273	.28402
2.3	-42.126	11.956	.91208	6.5542	.92173	17.032	.29727
2.4	-38.792	10.381	.82613	6.2829	.92281	17.792	.31053
2.5	-35.812	9.1113	.75527	6.0318	.92345	18.549	.32373
2.6	-33.154	8.0664	.6954	5.7998	.92382	19.301	.33687
2.7	-30.777	7.1883	.64355	5.5849	.92405	20.05	.34994
2.8	-28.64	6.4398	.59795	5.3849	.92419	20.798	.36299
2.9	-26.709	5.7995	.55785	5.1981	.92422	21.545	.37603
3	-24.967	5.2581	.5233	5.024	.92405	22.288	.38899

Table IV (continued). Dielectric Function and Optical Properties of Aluminum

Energy	Dielectric Function		Refractive Index		Reflectivity		
eV	ϵ_1	ϵ_2	n	k	R	θ (degrees)	θ (radians)
3.2	-21.951	4.3266	.45953	4.7077	.92433	23.774	.41494
3.4	-19.424	3.6058	.40734	4.4261	.92446	25.266	.44097
3.6	-17.288	3.0346	.36353	4.1737	.92458	26.762	.46709
3.8	-15.468	2.5754	.32629	3.9464	.9247	28.264	.4933
4	-13.901	2.2027	.29448	3.74	.9248	29.774	.51966
4.2	-12.545	1.8986	.26726	3.552	.92483	31.291	.54614
4.4	-11.366	1.6474	.24369	3.3801	.92486	32.813	.57269
4.6	-10.333	1.4374	.22304	3.2222	.92489	34.342	.59937
4.8	-9.4229	1.2603	.20483	3.0765	.92495	35.878	.6262
5	-8.6168	1.1199	.19036	2.9416	.92439	37.42	.65311
5.5	-6.9646	.81915	.15493	2.6436	.92554	41.327	.72129
6	-5.7	.62085	.12983	2.391	.92574	45.291	.79047
6.5	-4.7106	.47906	.11022	2.1732	.92597	49.327	.86092
7	-3.9229	.37529	.094632	1.9829	.92621	53.441	.93273
7.5	-3.2853	.2974	.081956	1.8144	.92654	57.647	1.0061
8	-2.7618	.23806	.071558	1.6634	.92689	61.958	1.0814
8.5	-2.3268	.19224	.06296	1.5267	.92723	66.388	1.1587
9	-1.9617	.15604	.05566	1.4017	.9277	70.953	1.2384
9.5	-1.6513	.12726	.04948	1.286	.92816	75.687	1.321
10	-1.386	.10421	.044227	1.1781	.92862	80.604	1.4068
10.5	-1.1566	.08517	.03957	1.0762	.9293	85.756	1.4967
11	-.95619	.069713	.035622	.9785	.92981	91.208	1.5919
11.5	-.77942	.058537	.033129	.88347	.92829	97.046	1.6938
12	-.6241	.051904	.032822	.79068	.9224	103.3	1.8029
12.5	-.48873	.048139	.034388	.69994	.91182	109.98	1.9195
13	-.37007	.045883	.03764	.6095	.89604	117.22	2.0459
13.25	-.31689	.044294	.039247	.5643	.88774	121.07	2.1131
13.5	-.26564	.042292	.0409	.51702	.87889	125.26	2.1862
13.75	-.21697	.04096	.043774	.46785	.86617	129.79	2.2652
14	-.17115	.040106	.048147	.4165	.8486	134.7	2.3509
14.1	-.15357	.03969	.05023	.39509	.84042	136.8	2.3876
14.2	-.13652	.03928	.052624	.37321	.83124	138.98	2.4256
14.3	-.11975	.038719	.055245	.35043	.82126	141.28	2.4658
14.4	-.10332	.038018	.058192	.32666	.81021	143.72	2.5083
14.5	-.086963	.037115	.0616	.30126	.79766	146.36	2.5544
14.55	-.078578	.036667	.063773	.28748	.78992	147.81	2.5797
14.6	-.070376	.036441	.066615	.27352	.78024	149.28	2.6055
14.65	-.062276	.036115	.069693	.2591	.76987	150.82	2.6323
14.7	-.053903	.035823	.073546	.24354	.75724	152.49	2.6615
14.75	-.045564	.035835	.078751	.22752	.74084	154.22	2.6916
14.8	-.037265	.036129	.085553	.21115	.72019	155.99	2.7226
14.85	-.029246	.036772	.094176	.19523	.69506	157.72	2.7527
14.9	-.021842	.037508	.10383	.18062	.66802	159.31	2.7805

Table IV (continued). Dielectric Function and Optical Properties of Aluminum

Energy	Dielectric Function		Refractive Index		Reflectivity		
eV	ϵ_1	ϵ_2	n	k	R	θ (degrees)	θ (radians)
14.95	-.01463	.03801	.11423	.16637	.63998	160.87	2.8077
15	-.0078247	.038338	.12511	.15322	.61187	162.31	2.8329
15.05	-6.4147E-4	.038274	.13718	.1395	.58197	163.82	2.8592
15.1	.0063188	.038521	.15059	.1279	.55055	165.09	2.8814
15.15	.013235	.038545	.1643	.1173	.52007	166.26	2.9017
15.2	.020186	.038548	.17846	.108	.49026	167.27	2.9195
15.25	.027228	.038589	.19295	.1	.46147	168.14	2.9347
15.3	.034102	.038856	.20712	.093799	.43484	168.81	2.9463
15.35	.040978	.039002	.22085	.0883	.41039	169.4	2.9565
15.4	.04769	.039414	.23405	.0842	.38809	169.82	2.964
15.45	.054251	.039731	.24647	.0806	.3681	170.19	2.9705
15.5	.060605	.040117	.25815	.0777	.35015	170.49	2.9756
15.55	.067038	.04026	.26948	.0747	.33345	170.79	2.9809
15.6	.073266	.040811	.2803	.0728	.3182	170.97	2.984
15.65	.079223	.041097	.29023	.0708	.30471	171.16	2.9874
15.7	.085171	.041258	.29984	.0688	.29213	171.36	2.9908
15.75	.091097	.041429	.30917	.067	.28034	171.53	2.9938
15.8	.096931	.041612	.31813	.0654	.2694	171.68	2.9964
15.85	.10267	.041756	.32673	.0639	.25924	171.82	2.9988
15.9	.10828	.041868	.33494	.0625	.24984	171.95	3.0011
15.95	.11384	.04183	.34287	.061	.24103	172.1	3.0036
16	.11946	.041735	.35071	.0595	.23256	172.24	3.0062
16.1	.13054	.041698	.36577	.057	.21701	172.47	3.0102
16.2	.14142	.041496	.38	.0546	.20309	172.7	3.0142
16.3	.15219	.041252	.39362	.052401	.19047	172.91	3.0178
16.4	.16288	.040997	.40672	.0504	.17893	173.09	3.021
16.5	.17342	.040837	.41928	.0487	.1684	173.24	3.0236
16.75	.19886	.040429	.44821	.0451	.146	173.54	3.0289
17	.22322	.04013	.47435	.0423	.12783	173.76	3.0326
17.25	.24648	.039846	.49808	.04	.11289	173.91	3.0354
17.5	.26864	.039601	.5197	.0381	.10045	174.03	3.0374
17.75	.28987	.039176	.53962	.0363	.089921	174.14	3.0393
18	.3103	.038846	.55813	.0348	.080881	174.22	3.0407
18.5	.34841	.038307	.59115	.0324	.066411	174.3	3.0422
19	.38348	.037448	.61999	.0302	.055353	174.39	3.0436
19.5	.41593	.036667	.64555	.0284	.04668	174.43	3.0444
20	.44595	.035822	.66833	.0268	.03977	174.46	3.0449
20.5	.47383	.034992	.68882	.0254	.034169	174.47	3.0451
21	.49974	.034235	.70734	.0242	.029578	174.46	3.0449
21.5	.52388	.033456	.72416	.0231	.025769	174.45	3.0446
22	.54638	.032834	.73951	.0222	.022534	174.4	3.0438
22.5	.56719	.032275	.75342	.021419	.019922	174.34	3.0427
23	.58665	.031402	.7662	.020492	.017654	174.33	3.0426

Table IV (continued). Dielectric Function and Optical Properties of Aluminum

Energy	Dielectric Function		Refractive Index		Reflectivity		
eV	ϵ_1	ϵ_2	n	k	R	θ (degrees)	θ (radians)
23.5	.60502	.030656	.77808	.0197	.015698	174.29	3.042
24	.62225	.02991	.78906	.018953	.014013	174.26	3.0414
24.5	.63846	.029252	.79925	.0183	.012551	174.21	3.0405
25	.65365	.028627	.80868	.0177	.011284	174.15	3.0396
25.5	.66792	.027957	.81744	.0171	.010177	174.11	3.0388
26	.68145	.027247	.82566	.0165	.0091995	174.08	3.0382
26.5	.69422	.026667	.83335	.016	.0083379	174.02	3.0371
27	.70622	.026056	.84051	.0155	.0075793	173.97	3.0363
27.5	.71758	.025417	.84723	.015	.0069048	173.93	3.0356
28	.72834	.024753	.85355	.0145	.0063033	173.9	3.0351
28.5	.73856	.024066	.85951	.014	.0057646	173.88	3.0347
29	.7483	.023359	.86515	.0135	.0052795	173.87	3.0346
29.5	.75762	.022633	.87051	.013	.0048404	173.87	3.0346
30	.76651	.02197	.8756	.012546	.004444	173.86	3.0344
31	.78344	.020453	.8852	.011553	.0037459	173.9	3.0352
32	.79896	.019902	.89391	.011132	.003172	173.67	3.0312
33	.8127	.01931	.90156	.010709	.0027114	173.47	3.0276
34	.82528	.018544	.90851	.010206	.0023268	173.33	3.0252
35	.83681	.017966	.91483	.0098194	.0020048	173.13	3.0217
36	.84746	.017168	.92062	.0093241	.0017316	173.02	3.0198
37	.85743	.016623	.92602	.0089755	.0014971	172.82	3.0162
38	.86649	.016225	.9309	.0087147	.0013012	172.55	3.0116
39	.87492	.015612	.93541	.008345	.0011324	172.39	3.0088
40	.88269	.015332	.93955	.0081592	9.8902E-4	172.07	3.0032
41	.88977	.014712	.94331	.0077981	8.6714E-4	171.94	3.0009
42	.89674	.013904	.94699	.0073411	7.5544E-4	171.9	3.0002
43	.90335	.01363	.95047	.0071701	6.5824E-4	171.55	2.9941
44	.90947	.01322	.95369	.006931	5.7454E-4	171.29	2.9895
45	.91527	.013043	.95672	.0068165	5.0132E-4	170.85	2.9819
46	.92029	.013109	.95934	.0068323	4.4276E-4	170.26	2.9716
47	.92502	.012314	.9618	.0064015	3.8978E-4	170.3	2.9723
48	.93006	.011719	.96442	.0060757	3.377E-4	170.13	2.9694
49	.93472	.011698	.96683	.0060497	2.9391E-4	169.49	2.9581
50	.9389	.011383	.96899	.0058737	2.5699E-4	169.1	2.9514
51	.9429	.011028	.97105	.0056784	2.2407E-4	168.74	2.945
52	.94695	.010423	.97313	.0053554	1.9284E-4	168.57	2.9422
53	.95101	.010237	.97521	.0052486	1.6456E-4	167.89	2.9303
54	.9547	.010157	.9771	.0051975	1.4105E-4	167.06	2.9158
55	.95813	.0099416	.97885	.0050782	1.2077E-4	166.35	2.9033
56	.96162	.0095412	.98063	.0048648	1.0163E-4	165.76	2.893
57	.96512	.0094322	.98242	.0048005	8.4532E-5	164.59	2.8726
58	.96828	.0094486	.98402	.004801	7.0696E-5	163.14	2.8472
59	.97131	.0091151	.98556	.0046243	5.8302E-5	162.11	2.8293

Table IV (continued). Dielectric Function and Optical Properties of Aluminum

Energy	Dielectric Function		Refractive Index		Reflectivity		
eV	ε_1	ε_2	n	k	R	θ (degrees)	θ (radians)
60	.97456	.0087087	.98721	.0044108	4.6364E-5	160.85	2.8073
61	.97784	.0085879	.98887	.0043423	3.6098E-5	158.57	2.7675
62	.98101	.0084568	.99047	.0042691	2.7529E-5	155.75	2.7183
63	.98424	.0082604	.9921	.0041631	2.0104E-5	152.1	2.6546
64	.98756	.0082042	.99377	.0041278	1.4053E-5	146.36	2.5544
65	.99067	.0083101	.99533	.0041745	9.8482E-6	138.07	2.4098
66	.99398	.0077765	.99699	.0039	6.0811E-6	127.52	2.2257
67	.99789	.007441	.99895	.0037244	3.7466E-6	105.62	1.8434
68	1.0021	.0073387	1.0011	.0036655	3.634E-6	73.821	1.2884
69	1.0068	.0072317	1.0034	.0036036	6.1168E-6	46.556	.81256
70	1.0125	.0070858	1.0062	.0035209	1.[illegible]744E-5	29.346	.51219
70.5	1.0159	.0070423	1.0079	.0034935	1.8604E-5	23.69	.41346
71	1.02	.0069815	1.01	.0034563	2.[illegible]495E-5	19.046	.33241
71.5	1.0254	.0068786	1.0126	.0033964	4.2204E-5	14.959	.26109
72	1.0329	.0070415	1.0163	.0034642	6.8486E-5	11.884	.20741
72.1	1.035	.0069488	1.0174	.0034151	7.6877E-5	11.035	.1926
72.2	1.0374	.0069398	1.0185	.0034068	8.7156E-5	10.319	.18009
72.3	1.0404	.0068713	1.02	.0033683	1.0086E-4	9.4615	.16513
72.4	1.0444	.006789	1.022	.0033215	1.207E-4	8.5053	.14844
72.5	1.0498	.0072644	1.0246	.003545	1.5074E-4	8.0986	.14135
72.6	1.0609	.0081393	1.03	.0039511	2.223E-4	7.3894	.12897
72.7	1.0688	.025492	1.0339	.012328	3.1455E-4	19.636	.34272
72.8	1.0609	.041175	1.0302	.019984	3.1805E-4	32.935	.57482
72.9	1.0511	.040888	1.0254	.019937	2.5445E-4	37.537	.65515
73	1.0489	.039105	1.0243	.019088	2.3341E-4	37.569	.6557
73.1	1.0516	.039983	1.0257	.019491	2.5304E-4	36.668	.63998
73.2	1.0504	.049549	1.0252	.024166	2.9688E-4	43.145	.75302
73.3	1.0431	.053085	1.0217	.02598	2.7981E-4	49.454	.86314
73.4	1.0376	.051766	1.0189	.025402	2.463E-4	52.566	.91744
73.5	1.0349	.050481	1.0176	.024804	2.2722E-4	53.933	.94131
73.6	1.0333	.049756	1.0168	.024467	2.166E-4	54.817	.95673
73.7	1.032	.049488	1.0162	.02435	2.1013E-4	55.729	.97265
73.8	1.0308	.049276	1.0156	.02426	2.0454E-4	56.613	.98809
73.9	1.0298	.049153	1.0151	.024211	2.0033E-4	57.396	1.0018
74	1.0289	.049041	1.0146	.024167	1.9664E-4	58.115	1.0143
74.5	1.0249	.049278	1.0127	.024331	1.8572E-4	61.807	1.0787
75	1.0221	.048564	1.0113	.024011	1.7392E-4	64.163	1.1199
75.5	1.0205	.04841	1.0105	.023954	1.6911E-4	65.684	1.1464
76	1.0197	.048178	1.0101	.023849	1.6591E-4	66.401	1.1589
76.5	1.0192	.049422	1.0099	.02447	1.7223E-4	67.374	1.1759
77	1.0175	.050823	1.009	.025184	1.773E-4	69.563	1.2141
77.5	1.0151	.051097	1.0078	.02535	1.7462E-4	72.09	1.2582
78	1.0139	.049871	1.0072	.024757	1.6507E-4	73.013	1.2743

Table IV (continued). Dielectric Function and Optical Properties of Aluminum

Energy	Dielectric Function		Refractive Index		Reflectivity		
eV	ϵ_1	ϵ_2	n	k	R	θ (degrees)	θ (radians)
79	1.0133	.049331	1.0069	.024496	1.6086E-4	73.513	1.283
80	1.0134	.04928	1.007	.024469	1.607E-4	73.391	1.2809
81	1.0137	.050077	1.0071	.024861	1.6603E-4	73.28	1.279
82	1.0137	.051293	1.0071	.025464	1.7361E-4	73.592	1.2844
83	1.0134	.052819	1.007	.026225	1.8294E-4	74.267	1.2962
84	1.0131	.054019	1.0069	.026825	1.904E-4	74.837	1.3062
85	1.0122	.055896	1.0065	.027768	2.0187E-4	76.102	1.3282
86	1.011	.056799	1.0059	.028233	2.0667E-4	77.427	1.3514
87	1.0103	.057308	1.0055	.028496	2.0948E-4	78.183	1.3645
88	1.01	.05823	1.0054	.028958	2.1574E-4	78.601	1.3718
89	1.0103	.059145	1.0056	.029409	2.2268E-4	78.441	1.3691
90	1.0098	.062184	1.0054	.030926	2.4492E-4	79.277	1.3836
91	1.0086	.063973	1.0048	.031834	2.5779E-4	80.524	1.4054
92	1.0068	.067059	1.0039	.033398	2.8156E-4	82.3	1.4364
93	1.0036	.069307	1.0024	.034571	2.9941E-4	85.048	1.4844
94	.99978	.070656	1.0005	.03531	3.1151E-4	88.156	1.5386
95	.99602	.071015	.99864	.035556	3.1685E-4	91.169	1.5912
96	.99149	.071495	.99638	.035877	3.2614E-4	94.729	1.6533
97	.98645	.069496	.99382	.034964	3.1704E-4	99.024	1.7283
98	.98315	.06559	.99209	.033056	2.9104E-4	102.51	1.7891
99	.98158	.062159	.99124	.031354	2.6721E-4	104.7	1.8274
100	.98036	.05927	.99058	.029917	2.482E-4	106.61	1.8607
101	.97965	.055683	.99017	.028118	2.2395E-4	108.46	1.8929
102	.98031	.052022	.99045	.026262	1.9704E-4	109.22	1.9062
103	.9824	.049291	.99147	.024857	1.7411E-4	108.22	1.8888
104	.9846	.048608	.99257	.024486	1.6488E-4	106.17	1.853
105	.98603	.0485	.99329	.024414	1.6132E-4	104.67	1.8268
106	.98695	.048709	.99376	.024508	1.6088E-4	103.59	1.808
107	.98773	.048885	.99415	.024586	1.6059E-4	102.68	1.7921
108	.98797	.049865	.99428	.025076	1.6629E-4	102.12	1.7824
109	.9876	.050249	.9941	.025274	1.6936E-4	102.41	1.7874
110	.98712	.050591	.99387	.025452	1.7238E-4	102.82	1.7946
111	.9865	.050668	.99355	.025498	1.7402E-4	103.45	1.8056
112	.98577	.0507	.99319	.025524	1.7564E-4	104.21	1.8188
113	.98502	.050375	.99281	.02537	1.7508E-4	105.1	1.8344
114	.98443	.049958	.9925	.025168	1.7367E-4	105.86	1.8477
115	.984	.049469	.99228	.024927	1.7153E-4	106.49	1.8586
116	.98369	.049125	.99212	.024758	1.7007E-4	106.94	1.8665
117	.98343	.048924	.99199	.02466	1.6941E-4	107.29	1.8726
118	.98271	.049133	.99163	.024774	1.7239E-4	107.96	1.8843
119	.98173	.048542	.99113	.024488	1.711E-4	109.22	1.9062
120	.98136	.047692	.99093	.024064	1.6683E-4	109.96	1.9192
122	.98064	.047368	.99056	.02391	1.6674E-4	110.85	1.9348

Table IV (continued). Dielectric Function and Optical Properties of Aluminum

Energy	Dielectric Function		Refractive Index		Reflectivity		
eV	ϵ_1	ϵ_2	n	k	R	θ (degrees)	θ (radians)
124	.97901	.046899	.98973	.023693	1.6839E-4	112.75	1.9678
126	.977	.045553	.9887	.023037	1.6644E-4	115.46	2.0152
128	.97541	.04327	.98787	.021901	1.5858E-4	118.35	2.0655
130	.97458	.040695	.98742	.020607	1.4754E-4	120.8	2.1084
132	.97449	.038093	.98735	.019291	1.3472E-4	122.7	2.1415
134	.97519	.035799	.98768	.018123	1.2152E-4	123.68	2.1586
136	.97595	.034553	.98806	.017485	1.1344E-4	123.83	2.1613
138	.97653	.033239	.98834	.016816	1.0591E-4	124.26	2.1687
140	.97719	.032247	.98866	.016308	9.9739E-5	124.33	2.17
142	.97775	.031516	.98894	.015934	9.5094E-5	124.3	2.1695
144	.97806	.030932	.98909	.015637	9.1861E-5	124.45	2.172
146	.97834	.030153	.98923	.015241	8.8018E-5	124.81	2.1784
148	.97879	.029505	.98945	.01491	8.4281E-5	124.85	2.1791
150	.97907	.029245	.98959	.014776	8.2529E-5	124.74	2.1771
152	.97912	.02886	.98961	.014581	8.0965E-5	125.05	2.1825
154	.97914	.028458	.98962	.014378	7.9441E-5	125.41	2.1889
156	.97904	.028143	.98957	.01422	7.8578E-5	125.86	2.1966
158	.97878	.027716	.98943	.014006	7.7777E-5	126.63	2.2101
160	.97848	.027176	.98928	.013735	7.6728E-5	127.58	2.2268
162	.97807	.026625	.98907	.01346	7.6005E-5	128.7	2.2463
164	.97758	.025778	.98881	.013035	7.4597E-5	130.26	2.2735
166	.97712	.024699	.98857	.012492	7.2483E-5	132.09	2.3054
168	.97704	.023151	.98852	.01171	6.7988E-5	134.09	2.3403
170	.97763	.021736	.98881	.010991	6.218E-5	135.19	2.3595
172	.9783	.021063	.98915	.010647	5.8413E-5	135.24	2.3604
174	.97882	.020357	.98941	.010287	5.5093E-5	135.54	2.3657
176	.97941	.019873	.9897	.01004	5.2245E-5	135.44	2.3638
178	.97963	.019745	.98981	.0099741	5.1336E-5	135.32	2.3617
180	.97973	.019128	.98986	.009662	4.9542E-5	136.1	2.3755
185	.98034	.017906	.99016	.009042	4.5075E-5	137.15	2.3938
190	.98095	.016795	.99047	.0084783	4.1087E-5	138.11	2.4105
195	.9815	.015839	.99074	.0079935	3.7764E-5	138.97	2.4255
200	.982	.014904	.99099	.0075198	3.4754E-5	139.94	2.4425
210	.98296	.013238	.99147	.006676	2.9602E-5	141.77	2.4744
220	.98385	.0118	.99191	.0059481	2.5412E-5	143.5	2.5046
230	.98468	.010495	.99232	.0052881	2.1887E-5	145.28	2.5357
240	.98546	.0093691	.99271	.0047189	1.8974E-5	146.93	2.5645
250	.98619	.0083246	.99308	.0041913	1.6478E-5	148.68	2.5949
260	.9869	.0073762	.99344	.0037125	1.4313E-5	150.4	2.625
270	.9876	.0065162	.99379	.0032785	1.2417E-5	152.09	2.6545
280	.98834	.0057075	.99416	.0028705	1.0657E-5	153.75	2.6835
290	.98912	.0051024	.99455	.0025652	9.1246E-6	154.73	2.7005
300	.98978	.0046841	.99488	.0023541	7.9807E-6	155.24	2.7095

Table IV (continued). Dielectric Function and Optical Properties of Aluminum

Energy	Dielectric Function		Refractive Index		Reflectivity		
eV	ϵ_1	ϵ_2	n	k	R	θ (degrees)	θ (radians)
310	.99036	.0042426	.99517	.0021316	7.0004E-6	156.12	2.7249
320	.99093	.0039202	.99546	.001969	6.1578E-6	156.51	2.7317
330	.99138	.0036804	.99568	.0018482	5.5383E-6	156.77	2.7362
340	.99174	.0034197	.99586	.001717	5.0367E-6	157.41	2.7473
350	.99206	.0031297	.99602	.0015711	4.5888E-6	158.4	2.7645
360	.99239	.0028304	.99619	.0014206	4.1518E-6	159.52	2.7841
370	.99273	.0025299	.99636	.0012696	3.7304E-6	160.74	2.8054
380	.9931	.0022719	.99654	.0011399	3.3211E-6	161.71	2.8224
390	.99346	.0020768	.99673	.0010418	2.9621E-6	162.32	2.8331
400	.99378	.0019393	.99689	9.7268E-4	2.6697E-6	162.63	2.8384
420	.9943	.0016764	.99715	8.406E-4	2.2189E-6	163.56	2.8547
440	.99476	.0014294	.99738	7.1658E-4	1.8535E-6	164.7	2.8746
460	.99517	.0012151	.99758	6.0902E-4	1.5579E-6	165.84	2.8945
480	.99555	.0010221	.99777	5.1219E-4	1.3088E-6	167.03	2.9153
500	.9959	8.6947E-4	.99795	4.3563E-4	1.1024E-6	168	2.9322
520	.9962[illegible]	7.5181E-4	.9981	3.7662E-4	9.3663E-7	168.76	2.9454
540	.99649	6.5099E-4	.99824	3.2607E-4	7.993E-7	169.47	2.9579
560	.99675	5.6194E-4	.99837	2.8143E-4	6.8211E-7	170.17	2.9701
580	.99697	4.9781E-4	.99848	2.4928E-4	5.9108E-7	170.66	2.9785
600	.99717	4.408E-4	.99858	2.2071E-4	5.1415E-7	171.13	2.9869
620	.99736	3.8461E-4	.99868	1.9256E-4	4.4602E-7	171.7	2.9967
640	.99753	3.4088E-4	.99876	1.7065E-4	3.8953E-7	172.13	3.0043
660	.99768	2.9947E-4	.99884	1.4991E-4	3.428E-7	172.64	3.0131
680	.99782	2.5978E-4	.99891	1.3003E-4	3.019E-7	173.2	3.0229
700	.99796	2.363E-4	.99898	1.1827E-4	2.6413E-7	173.39	3.0262
720	.99808	2.1825E-4	.99904	1.0923E-4	2.3383E-7	173.51	3.0283
740	.99818	1.9743E-4	.99909	9.8805E-5	2.0984E-7	173.8	3.0334
760	.99828	1.7978E-4	.99914	8.9967E-5	1.8724E-7	174.03	3.0374
780	.99837	1.6247E-4	.99918	8.1301E-5	1.6798E-7	174.3	3.0422
800	.99845	1.4621E-4	.99922	7.3162E-5	1.5173E-7	174.61	3.0475
820	.99853	1.3122E-4	.99926	6.5658E-5	1.3633E-7	174.9	3.0525
840	.99861	1.194E-4	.9993	5.9742E-5	1.2182E-7	175.09	3.0558
860	.99868	1.1243E-4	.99934	5.6252E-5	1.0983E-7	175.13	3.0566
880	.99874	1.0364E-4	.99937	5.1853E-5	1.0002E-7	175.29	3.0595
900	.99879	9.3552E-5	.99939	4.6804E-5	9.2165E-8	175.58	3.0644
920	.99885	8.3934E-5	.99942	4.1991E-5	8.3192E-8	175.82	3.0687
940	.9989	7.6636E-5	.99945	3.8339E-5	7.6076E-8	176.01	3.072
960	.99895	7.2676E-5	.99947	3.6357E-5	6.9309E-8	176.04	3.0725
980	.999	6.7984E-5	.9995	3.4009E-5	6.2852E-8	176.11	3.0737
1000	.99904	6.222E-5	.99952	3.1125E-5	5.7898E-8	176.29	3.0768
1050	.99914	5.1058E-5	.99957	2.554E-5	4.6428E-8	176.6	3.0823
1100	.99922	4.3115E-5	.99961	2.1566E-5	3.8171E-8	176.83	3.0864
1150	.9993	3.6069E-5	.99965	1.8041E-5	3.0728E-8	177.05	3.0901

Table IV (continued). Dielectric Function and Optical Properties of Aluminum

Energy	Dielectric Function		Refractive Index		Reflectivity		
eV	ϵ_1	ϵ_2	n	k	R	θ (degrees)	θ (radians)
1200	.99936	3.119E-5	.99968	1.56E-5	2.5677E-8	177.21	3.0929
1250	.99942	2.6992E-5	.99971	1.35E-5	2.1083E-8	177.33	3.0951
1300	.99947	2.3194E-5	.99973	1.16E-5	1.7599E-8	177.49	3.0978
1350	.99952	1.9995E-5	.99976	9.9999E-6	1.4432E-8	177.61	3.1
1400	.99957	1.7796E-5	.99978	8.8999E-6	1.1581E-8	177.63	3.1002
1450	.99961	1.5597E-5	.9998	7.8E-6	9.5252E-9	177.71	3.1016
1500	.99966	1.3558E-5	.99983	6.7802E-6	7.2389E-9	177.72	3.1017
1510	.99968	1.3238E-5	.99984	6.6201E-6	6.413E-9	177.63	3.1002
1520	.99969	1.2898E-5	.99984	6.45E-6	6.0185E-9	177.62	3.1
1530	.99971	1.2598E-5	.99985	6.2999E-6	5.2677E-9	177.51	3.0982
1540	.99974	1.2298E-5	.99987	6.1498E-6	4.2356E-9	177.29	3.0943
1542	.99974	1.2238E-5	.99987	6.1198E-6	4.2355E-9	177.3	3.0946
1544	.99975	1.2178E-5	.99987	6.0898E-6	3.9165E-9	177.21	3.0929
1546	.99976	1.2119E-5	.99988	6.0602E-6	3.61E-9	177.11	3.0911
1548	.99977	1.2059E-5	.99988	6.0302E-6	3.3161E-9	177	3.0892
1549	.99977	1.2019E-5	.99988	6.0102E-6	3.316E-9	177.01	3.0894
1550	.99978	1.1999E-5	.99989	6.0002E-6	3.0347E-9	176.88	3.0871
1551	.99979	1.1979E-5	.99989	5.9901E-6	2.7658E-9	176.73	3.0846
1552	.9998	1.1939E-5	.9999	5.9701E-6	2.5094E-9	176.58	3.082
1553	.99982	1.6572E-5	.99991	8.2867E-6	2.0425E-9	174.74	3.0498
1554	.99983	3.9355E-5	.99991	1.9679E-5	1.9034E-9	166.96	2.9141
1555	.99983	5.9093E-5	.99991	2.9549E-5	2.0248E-9	160.83	2.807
1556	.99982	6.2094E-5	.99991	3.105E-5	2.2664E-9	160.97	2.8094
1557	.99983	5.8603E-5	.99991	2.9304E-5	2.0212E-9	160.98	2.8096
1558	.99984	6.5831E-5	.99992	3.2918E-5	1.8712E-9	157.63	2.7512
1559	.99985	8.2294E-5	.99992	4.115E-5	1.8298E-9	151.25	2.6398
1560	.99985	1.0003E-4	.99992	5.0019E-5	2.0319E-9	146.3	2.5534
1561	.99985	1.2198E-4	.99992	6.0995E-5	2.3365E-9	140.88	2.4588
1562	.99985	1.4371E-4	.99992	7.186E-5	2.6974E-9	136.22	2.3775
1563	.99983	1.6362E-4	.99991	8.1817E-5	3.4801E-9	136.09	2.3752
1564	.99981	1.7089E-4	.9999	8.5453E-5	4.0822E-9	138.03	2.409
1565	.99979	1.686E-4	.99989	8.4309E-5	4.5338E-9	141.24	2.465
1566	.99978	1.6598E-4	.99989	8.2949E-5	4.7458E-9	142.98	2.4955
1567	.99978	1.6565E-4	.99989	8.2834E-5	4.741E-9	143.02	2.4961
1568	.99977	1.6414E-4	.99988	8.2079E-5	4.9913E-9	144.48	2.5217
1569	.99976	1.6364E-4	.99988	8.183E-5	5.2749E-9	145.71	2.5431
1570	.99976	1.6222E-4	.99988	8.112E-5	5.246E-9	145.94	2.5471
1575	.99974	1.5969E-4	.99987	7.9855E-5	5.8203E-9	148.44	2.5907
1580	.99973	1.5697E-4	.99986	7.8496E-5	6.0979E-9	149.82	2.6149
1585	.99972	1.5438E-4	.99986	7.7201E-5	6.3914E-9	151.13	2.6376
1590	.99971	1.5197E-4	.99985	7.5996E-5	6.7016E-9	152.34	2.6588
1595	.99971	1.4955E-4	.99985	7.4786E-5	6.656E-9	152.72	2.6654
1600	.9997	1.4762E-4	.99985	7.3321E-5	6.9891E-9	153.8	2.6842

Table IV (continued). Dielectric Function and Optical Properties of Aluminum

Energy	Dielectric Function		Refractive Index		Reflectivity		
eV	ϵ_1	ϵ_2	n	k	R	θ (degrees)	θ (radians)
1610	.9997	1.4434E-4	.99985	7.2131E-5	6.9292E-9	154.3	2.6931
1620	.99969	1.4084E-4	.99984	7.0431E-5	7.2482E-9	155.56	2.7151
1630	.99969	1.3757E-4	.99984	6.8796E-5	7.1913E-9	156.07	2.7239
1640	.99968	1.342E-4	.99984	6.7111E-5	7.528E-9	157.24	2.7444
1650	.99968	1.3093E-4	.99984	6.5475E-5	7.4738E-9	157.74	2.7532
1660	.99968	1.2769E-4	.99984	6.3855E-5	7.4214E-9	158.24	2.7619
1670	.99968	1.2448E-4	.99984	6.225E-5	7.3708E-9	158.74	2.7705
1680	.99968	1.2135E-4	.99984	6.0685E-5	7.3227E-9	159.23	2.7791
1690	.99968	1.186E-4	.99984	5.9309E-5	7.2815E-9	159.66	2.7866
1700	.99968	1.1586E-4	.99984	5.7939E-5	7.2413E-9	160.09	2.7942
1750	.99969	1.0421E-4	.99984	5.2113E-5	6.6871E-9	161.42	2.8172
1800	.9997	9.4264E-5	.99985	4.7139E-5	6.1822E-9	162.55	2.8371
1850	.99971	8.5018E-5	.99985	4.2515E-5	5.7097E-9	163.66	2.8564
1900	.99972	7.6913E-5	.99986	3.8462E-5	5.2712E-9	164.64	2.8735
1950	.99973	7.014E-5	.99986	3.5075E-5	4.865E-9	165.44	2.8874
2000	.99974	6.4056E-5	.99987	3.2032E-5	4.4826E-9	166.16	2.9
2200	.99978	4.2995E-5	.99989	2.15E-5	3.1412E-9	168.94	2.9486
2400	.99981	3.1597E-5	.9999	1.58E-5	2.3191E-9	170.56	2.9768
2600	.99984	2.3398E-5	.99992	1.17E-5	1.6345E-9	171.68	2.9964
2800	.99986	1.7999E-5	.99993	9.0001E-6	1.2454E-9	172.67	3.0137
3000	.99988	1.4199E-5	.99994	7.0999E-6	9.1271E-10	173.25	3.0238
3200	.99989	1.0999E-5	.99994	5.4998E-6	7.639E-10	174.29	3.0419
3400	.9999	8.8996E-6	.99995	4.45E-6	6.3001E-10	174.91	3.0528
3600	.99991	7.1997E-6	.99995	3.6E-6	5.0954E-10	175.43	3.0618
3800	.99992	5.8998E-6	.99996	2.95E-6	4.0221E-10	175.78	3.068
4000	.99993	4.8998E-6	.99996	2.45E-6	3.0777E-10	176	3.0717
4200	.99994	4.0999E-6	.99997	2.05E-6	2.2606E-10	176.09	3.0734
5000	.99996	2.08E-6	.99998	1.04E-6	1.0027E-10	177.02	3.0896
6000	.99997	1.046E-6	.99998	5.2301E-7	5.632E-11	178	3.1067
7000	.99998	5.7999E-7	.99999	2.9E-7	2.5022E-11	178.34	3.1126
8000	.99998	3.4E-7	.99999	1.7E-7	2.5008E-11	179.03	3.1246
9000	.99999	2.16E-7	.99999	1.08E-7	6.253E-12	178.76	3.12
10000	.99999	1.42E-7	.99999	7.1E-8	6.2513E-12	179.19	3.1274

ACKNOWLEDGMENTS

We are indebted to Professor Wayne Major of the University of Richmond for providing us with his reflectance measurement for a commercially supplied aluminum reflector and to Professor S. E. Schnatterly of the University of Virginia for helpful discussions.

REFERENCES

1. H. Ehrenreich, H. R. Philipp, and B. Segall, Phys. Rev. 132, 1918 (1963).
2. H. R. Philipp and H. Ehrenreich, J. Appl. Phys. 35, 1416 (1964).
3. C. J. Powell, J. Opt. Soc. Am. 60, 78 (1970).
4. T. Sasaki and M. Inokuti, Conference Digest of the Third International Conference on Vacuum Ultraviolet Radiation Physics, edited by Y. Nakai, Phys. Soc. of Japan, Tokyo (1971), p. 2aC2-2.
5. A. G. Mathewson and H. P. Myers, J. Phys. F 2, 403 (1972).
6. H.-J. Hagemann, W. Gudat, and C. Kunz, J. Opt. Soc. Am. 65, 742 (1975); and DESY Report SR 74/7, Hamburg (1974).
7. E. Shiles, T. Sasaki, M. Inokuti, and D. Y. Smith, Phys. Rev. B 22, 1612 (1980).
8. See, for example, F. Wooten, Optical Properties of Solids, Academic Press, New York (1972) sec. 3.2.
9. J. N. Hodgson, Proc. Phys. Soc. London, Sec. B 68, 593 (1955).
10. J. R. Beattie, Physica (Utrecht) 23, 898 (1957).
11. H. E. Bennett and J. M. Bennett, in Optical Properties and Electronic Structure of Metals and Alloys, edited by F. Abelès North-Holland, Amsterdam (1966), p. 175.
12. G. Dresselhaus, M. S. Dresselhaus, and D. Beaglehole, in Electronic Density of States, edited by L. H. Bennett, NBS Special Publication 323, National Bureau of Standards, Washington, D.C. (1971).
13. R. L. Benbow and D. W. Lynch, Phys. Rev. B 12, 5615 (1975).
14. D. Y. Smith and B. Segall, Bull. Am. Phys. Soc. 26, 209 (1981); D. Y. Smith, D. D. Koelling, and B. Segall, Bull. Am. Phys. Soc. 28, 387 (1983).
15. N. W. Ashcroft and K. Sturm, Phys. Rev. B 3, 1898 (1971).

16. W. A. Harrison, Phys. Rev. 147, 467 (1966).
17. A. I. Golováshkin, A. I. Kopeliovich, and G. P. Motulevich, Zh. Eksperim. i Teor. Fiz. 53, 2053 (1967) [English translation in Soviet Phys. JETP 26, 1161 (1968)].
18. N. W. Ashcroft, Phil. Mag. 8, 2055 (1963).
19. D. Brust, Phys. Rev. B 2, 818 (1970).
20. F. Szmulowicz and B. Segall, Phys. Rev. B 24, 892 (1981).
21. J. Strong, Astrophys. J. 83, 401 (1936).
22. L. G. Schulz, J. Opt. Soc. Am. 44, 357 (1954); L. G. Schulz and F. R. Tangherlini, ibid. 44, 362 (1954).
23. I. N. Shklyarevskii and R. G. Yarovaya, Opt. Spektrosk. 16, 85 (1964) [English translation in Opt. Spectrosc. (USSR) 16, 45 (1964)].
24. J. R. Beattie, Phil. Mag. 46, 235 (1955).
25. H. E. Bennett, M. Silver, and E. J. Ashley, J. Opt. Soc. Am. 53, 1089 (1963).
26. L. W. Bos and D. W. Lynch, Phys. Rev. Lett. 25, 156 (1970).
27. O. Hunderi and P. O. Nilsson, Solid State Commun. 19, 921 (1976); Nuovo Cimento 39 B, 459 (1977).
28. G. Quincke, Pogg. Ann. Jublbd. 336 (1874), evaluated by W. Voigt, Ann. Physik 23, 142 (1884) and F. F. Martens, Landolt-Börnstein, 5th edition, J. Springer, Berlin (1923) vol. 2, section 165, pg. 906.
29. P. Drude, Wied. Ann. 39, 481 (1890).
30. P. G. Nutting, Phys. Rev. 13, 193 (1901).
31. W. W. Coblentz, Bull. U.S. Bur. Stand. 2, 457 (1906).
32. W. v. Uljain, Physikal. Zeit. 11, 784 (1910).
33. M. Luckiesh, J. Opt. Soc. Am. 19, 1 (1929).
34. W. W. Coblentz and R. Stair, U.S. Bureau of Standards J. of Research 4, 189 (1930).
35. J. Wulff, J. Opt. Soc. Am. 24, 223 (1934).
36. A. H. Taylor, J. Opt. Soc. Am. 24, 192 (1934).
37. W. R. Grove, Phil. Trans., 87 (1852); W. Crookes, Proc. Roy. Soc. London 50, 88 (1891).
38. P. Pringsheim and R. Pohl, Verh. der Deut. Phys. Ges. 14, 506 (1912).
39. E. O. Hulburt, Astrophys. J. 42, 203 (1915).
40. P. R. Gleason, Proc. Nat. Acad. Sci. (USA) 15, 551 (1929).

41. R. Ritschl, Tätigkeitsbericht d. Phys. Techn. Reichsanstalt (1928); and Z. Phys. 69, 578 (1931).
42. J. Strong, Phys. Rev. 43, 498 (1933).
43. G. Hass, J. Opt. Soc. Am. 45, 945 (1955).
44. J. C. Burridge, H. Kuhn, and A. Pery, Proc. Phys. Soc. London, Sec. B 66, 963 (1953).
45. J. Halford, F. K. Chin, and J. E. Norman, J. Opt. Soc. Am. 63, 786 (1973).
46. G. Hass and J. E. Waylonis, J. Opt. Soc. Am. 51, 719 (1961).
47. E. T. Hutcheson, G. Hass, and J. K. Coulter, Opt. Commun. 3, 213 (1971).
48. J. G. Endriz and W. E. Spicer, Phys. Rev. B 4, 4144 (1971).
49. P. C. Gibbons, S. E. Schnatterly, J. J. Ritsko, and J. R. Fields, Phys. Rev. B 13, 2451 (1976).
50. R. W. Ditchburn and G. H. Freeman, Proc. Roy. Soc. London, Ser. A 294, 20 (1966).
51. T. Sasaki (private communication) and sources cited in Ref. 7.
52. G. Hass, Optik 1, 8 (1946).
53. G. B. Sabine, Phys. Rev. 55, 1064 (1939).
54. M. Banning, Phys. Rev. 59, 914 (1941); J. Opt. Soc. Am. 32, 98 (1942).
55. W. C. Walker, J. A. R. Samson, and O. P. Rustig, J. Opt. Soc. Am. 48, 71 (1958); W. C. Walker, O. P. Rustig, and G. L. Weissler, J. Opt. Soc. Am. 49, 471 (1959).
56. V. R. Weidner and J. J. Hsia, NBS Certificate for Standard Reference Material 2003a, National Bureau of Standards, Washington, D.C. (1981).
57. W. Major (Private communication). The commercial mirror consisted of a first-surface evaporated-aluminum-film (~1000 Å) reflector on optical glass prepared by D. and E. Technology, Santa Clara, California. The evaporation was performed at ~10^{-6} Torr.
58. For references to additional measurements see Ref. 7 and H. Schopper in Landolt-Börnstein Zahlenwerte und Funktionen, 6th edition, edited by J. Bartels et al., Springer, Berlin (1962), Vol. II, part 8, Optische Konstanten, Sec. 281, pp. 1-1 to 1-41. See also, R. C. Williams and G. O. Sabine, Astrophys. J. 77, 316 (1933); H. S. Jones, Nature 133, 552 (1934); B. K. Johnson, Nature, 134, 216 (1934); M.Auwärter, Z. Tech. Phys. 18, 457 (1937); B. K. Johnson, Proc. Phys. Soc. London 53, 258 (1941); A. Boettcher, Z. Angew. Phys. 2, 340 (1950).
59. G. Hass, Z. Anorg. Allg. Chem. 254, 96 (1947).

60. P. H. Berning, G. Hass, and R. P. Madden, J. Opt. Soc. Am. 50, 586 (1960).
61. I. N. Shklyarevskii and R. G. Yarovaya, Opt. Spektrosk. 14, 252 (1963) [English translation in Opt. Spectrosc. (USSR) 14, 130 (1963)].
62. R. W. Fane and W. E. J. Neal, J. Opt. Soc. Am. 60, 790 (1970).
63. J. Shewchun and E. C. Rowe, J. Appl. Phys. 41, 4128 (1970).
64. B. P. Feuerbacher and W. Steinmann, Opt. Commun. 1, 81 (1969).
65. A. Daude, A. Savary, and S. Robin, Thin Solid Films 13, 255 (1972); J. Opt. Soc. Am. 62, 1 (1972).
66. W. Walkenhorst, Z. Tech. Phys. 22, 14 (1941).
67. R. S. Sennett and G. D. Scott, J. Opt. Soc. Am. 40, 203 (1950); and M. F. Crawford, W. M. Gray, A. L. Schawlow, and F. M. Kelly, J. Opt. Soc. Am. 39, 888 (1949).
68. W. E. J. Neal, R. W. Fane, and N. W. Grimes, Phil. Mag. 21, 167 (1970).
69. R. P. Madden and L. R. Canfield, J. Opt. Soc. Am. 51, 838 (1961).
70. R. P. Madden, L. R. Canfield, and G. Hass, J. Opt. Soc. Am. 53, 620 (1963).
71. R. K. Hart, Proc. Roy. Soc. London, Sec. A 236, 68 (1956).
72. G. Hass, Ann. Phys. (Leipzig) 31, 245 (1938).
73. G. Hass, W. R. Hunter, and R. Tousey, J. Opt. Soc. Am. 46, 1009 (1956); 47, 1070 (1957).
74. R. P. Chasmar, J. L. Craston, G. Isaacs, and A. S. Young, J. Sci. Inst. 28, 206 (1951).
75. G. H. C. Freeman, Brit. J. Appl. Phys. 16, 927 (1965); E. T. Arakawa and M. W. Williams, J. Phys. Chem. Sol. 29, 735 (1968).
76. G. Hass and H. W. Scott, J. Opt. Soc. Am. 39, 179 (1949); W. R. Hunter, Optica Acta 9, 255 (1963); A. P. Bradford and G. Hass, J. Opt. Soc. Am. 53, 1096 (1963).
77. L. Holland, Vacuum Deposition of Thin Films, J. Wiley, New York (1958).
78. D. H. Tomboulian and E. M. Pell, Phys. Rev. 83, 1196 (1951).
79. A. Balzarotti, A. Bianconi, and E. Burattini, Phys. Rev. B 9, 5003 (1974).
80. J. M. Elson and R. H. Ritchie, Phys. Rev. B 4, 4129 (1971).
81. R. H. Ritchie and R. E. Wilems, Phys. Rev. 178, 372 (1969); J. Crowell and R. H. Ritchie, J. Opt. Soc. Am. 60, 794 (1970); J. M. Elson and R. H. Ritchie, Phys. Lett. 33A, 255 (1970).
82. R. C. Vehse, E. T. Arakawa, and J. L. Stanford, J. Opt. Soc. Am. 57, 551 (1967).

83. M. W. Williams, E. T. Arakawa, and L. C. Emerson, Surface Science 6, 127 (1967).

84. J. C. Miller, Phil. Mag. 20, 1115 (1969).

85. T. E. Faber, in Optical Properties and Electronic Structure of Metals and Alloys, edited by F. Abelès, North-Holland, Amsterdam (1966) p. 259.

86. L. G. Bernland, O. Hunderi, and H. P. Myers, Phys. Rev. Lett. 31, 363 (1973).

87. A. G. Mathewson and H. P. Myers, Physica Scripta 4, 291 (1971).

88. H. G. Liljenvall, A. G. Mathewson, and H. P. Myers, Solid State Commun. 9, 169 (1971).

89. R. Haensel, B. Sonntag, C. Kunz, and T. Sasaki, J. Appl. Phys. 40, 3046 (1969).

90. C. Gähwiller and F. C. Brown, Phys. Rev. B 2, 1918 (1970).

91. V. A. Fomichev and A. P. Lukirskii, Opt. Spektrosk. 22, 796 (1967) [English translation in Opt. Spectrosc. (USSR) 22, 432 (1967)].

92. V. A. Fomichev and A. P. Lukirskii, Fiz. Tverd. Tela 8, 2104 (1966) [English translation in Sov. Phys. - Solid State 8, 1674 (1967)].

93. V. A. Fomichev, Fiz. Tverd. Tela 8, 2892 (1966) [English translation in Sov. Phys. - Solid State 8, 2312 (1967)].

94. S. Singer, J. Appl. Phys. 38, 2897 (1967).

95. O. A. Ershov, I. A. Brytov, and A. P. Lukirskii, Opt. Spektrosk. 22, 127 (1967) [English translation in Opt. Spectrosc. (USSR) 22, 66 (1967)].

96. O. A. Ershov and I. A. Brytov, Opt. Spektrosk. 22, 305 (1967) [English translation in Opt. Spectrosc. (USSR) 22, 165 (1967)].

97. B. A. Cooke and E. A. Stewardson, Br. J. Appl. Phys. 15, 1315 (1964).

98. A. J. Bearden, J. Appl. Phys. 37, 1681 (1966).

99. B. L. Henke and R. L. Elgin, in Advances in X-Ray Analysis, edited by B. L. Henke, J. B. Newkirk, and G. R. Mallett, Plenum, New York (1970), Vol. 13, p. 639.

100. B. L. Henke and E. S. Ebisu, in Advances in X-Ray Analysis, edited by C. L. Grant, C. S. Barrett, J. B. Newkirk, and C. O. Ruud, Plenum, New York (1974), Vol. 17, p. 150.

101. L. Singman, J. Appl. Phys. 45, 1885 (1974).

102. P. Lublin, P. Cukor, and R. J. Jaworowski, in Advances in X-Ray Analysis, edited by B. L. Henke, J. B. Newkirk, and G. R. Mallett, Plenum, New York (1970), Vol. 13, p. 632.

103. J. H. Hubbell, W. H. McMaster, N. K. Del Grande, and J. H. Mallett, in International Tables for X-Ray Crystallography, edited by J. A. Ibers and W. C. Hamilton, Kynoch, Birmingham, England (1974), Vol. IV, p. 47.

104. C. M. Davisson, "Interaction of γ-Radiation with Matter" in Alpha-, Beta-, and Gamma-Ray Spectroscopy, edited by K. Siegbahn, North-Holland, Amsterdam (1965), Vol. I, p. 37.

105. A. P. Lukirskii, E. P. Savinov, O. A. Ershov, and Yu. F. Shepelev, Opt. Spektrosk. 16, 310 (1964) [English translation in Opt. Spectrosc. (USSR) 16, 168 (1964)].

106. A. Smakula, Z. Phys. 88, 114 (1934).

107. W. Woltersdorff, Z. Phys. 91, 230 (1934).

108. H. M. O'Bryan, J. Opt. Soc. Am. 26, 122 (1936).

109. K. B. Hunt, Investigations of the Reflectivity and Transmissivity of Selected Materials in the Infrared Region, MS Thesis, Purdue University (1945).

110. A. I. Golovashkin, G. P. Motulevich, and A. A. Shubin, Zh. Eksp. Teor. Fiz. 38, 51 (1960) [English translation in Sov. Phys. - JETP 11, 38 (1960)].

111. T. T. Cole and F. Oppenheimer, Appl. Opt. 1, 709 (1962).

112. W. R. Hunter, J. Appl. Phys. 34, 1565 (1963); J. Opt. Soc. Am. 54, 208 (1964); J. Phys. (Paris) 25, 154 (1964).

113. G. P. Motulevich, A. A. Shubin, and O. F. Shustova, Zh. Eksp. Teor. Fiz. 49, 1431 (1965) [English translation in Sov. Phys. - JETP 22, 984 (1966)].

114. A. P. Lenham and D. M. Terherne, J. Opt. Soc. Am. 56, 752 (1966).

115. A. Daude, M. Priol, and S. Robin, C. R. Acad. Sci. (Paris) B 263, 1178 (1966).

116. A. Daude, A. Savary, G. Jezequel, and S. Robin, C. R. Acad. Sci. (Paris) B 269, 901 (1969).

117. R. Haensel, G. Keitel, B. Sonntag, C. Kunz, and P. Schreiber, Phys. Status Solidi A 2, 85 (1970).

118. S. Kiyono, S. Chiba, Y. Hayasi, S. Kato, and S. Mochimaru, Jpn. J. Appl. Phys. Suppl. 17, Supplement 17-2, 212 (1978).

119. J. J. Hopfield, Phys. Rev. 139, A419 (1965).

120. K. L. Kliewer and R. Fuchs, Phys. Rev. 172, 607 (1968).

121. H. J. Levinson and E. W. Plummer, Phys. Rev. B 24, 628 (1981).

122. R. Rosei and D. W. Lynch, Phys. Rev. B 5, 3883 (1972).

123. S. D. Pudkov, Zh. Tehh. Fiz. 47, 649 (1977) [English translation in Sov. Phys. - Tech. Phys., 22, 389 (1977)].

124. Handbook of Chemistry and Physics, 58th ed., edited by R. C. Weast, CRC Press, Cleveland (1977).

125. G. T. Meaden, Electrical Resistance of Metals, Plenum, New York (1965).

Distribution for ANL-83-24

Internal:

J. Berkowitz
J. L. Dehmer
F. Y. Fradin
B. R. T. Frost
P. F. Gustafson
R. H. Huebner
M. Inokuti (40)
K. L. Kliewer
D. Y. Smith (40)
E. M. Stefanski
B. W. Veal
H. Wiedersich
ANL Patent Dept.
ANL Contract File
ANL Libraries
TIS Files (6)

External:

DOE-TIC, for distribution per UC-34 (95)
Manager, Chicago Operations Office, DOE
L. C. Ianniello, Office of Energy Research, DOE
M. C. Wittels, Office of Energy Research, DOE
Environmental Research Division Review Committee:
    A. K. Blackadar, Pennsylvania State U.
    A. W. Castleman, Jr., Pennsylvania State U.
    R. E. Gordon, U. Notre Dame
    R. A. Hites, Indiana U.
    D. Kleppner, Massachusetts Inst. Technology
    G. M. Matanoski, Johns Hopkins U.
    R. A. Reck, General Motors Research Lab.
    L. A. Sagan, Electric Power Research Inst.
    R. E. Wildung, Battelle Pacific Northwest Lab.
Materials Science and Technology Division Review Committee:
    C. B. Alcock, University of Toronto, Canda
    A. Arrott, Simon Fraser University, Burnaby, B. C., Canada
    R. C. Dynes, Bell Laboratories, Murray Hill, NJ
    A. G. Evans, University of California, Berkeley, CA
    L. M. Falicov, University of California, Berkeley, CA
    H. K. Forsen, Bechtel Group, Inc., San Francisco, CA
    E. Kay, IBM Research Laboratory, San Jose, CA
    M. B. Maple, University of California, LaJolla, CA
    C. L. McCabe, Cabot Corp., Kokomo, IN
    P. G. Shewmon, Ohio State University, Columbus, OH
    J. K. Tien, Columbia University, New York, NY
J. C. Ashley, Oak Ridge National Laboratory
M. J. Berger, National Bureau of Standards, Washington, DC
H. E. Bennett, Naval Weapons Center, China Lake, CA
H. Bichsel, Seattle, WA
J. W. Cooper, National Bureau of Standards, Washington, DC
B. Crasemann, University of Oregon, Eugene, OR
S. Datz, Oak Ridge National Laboratory
U. Fano, University of Chicago, Chicago, IL
F. P. Hudson, Office of Health and Environmental Research, USDOE
M. N. Kabler, U. S. Naval Research Laboratory, Washington, DC
M. O. Krause, Oak Ridge National Laboratory
C. E. Kuyatt, National Bureau of Standards, Washington, DC
D. W. Lynch, Iowa State University, Ames, IA
R. P. Madden, National Bureau of Standards, Washington, DC

F. A. Modine, Oak Ridge National Laboratory
L. R. Painter, University of Tennessee, Knoxville, TN
C. J. Powell, National Bureau of Standards, Washington, DC
R. H. Ritchie, Oak Ridge National Laboratory
S. E. Schnatterly, University of Virginia, Charlottesville, VA
E. Shiles, Gulf Research and Development Co., Houston, TX (10)
D. A. Shirley, University of California, Berkeley, CA
L. H. Toburen, Battelle Northwest Laboratory
J. E. Turner, Oak Ridge National Laboratory
R. W. Wood, Office of Health and Environmental Research, USDOE
D. Charlton, Concordia University, Montreal, Canada
J. Lindhard, Aarhus University, Denmark
P. Sigmund, Odense University, Denmark
J-P. Briand, Lab. de Physique Atomique et Nucleaire, Paris, France
F. Wuilleumier, Université Paris-Sud, Orsay, France
J. Booz, Institut für Medizin, Jülich, Germany
J. Geiger, Universität Kaiserslautern, Germany
R. Haensel, Universität Kiel, Germany
W. Mehlhorn, Universität Freiburg, Germany
H. Paus, Universität Stuttgart, Germany
H. Schmoranzer, Universität Kaiserslautern, Germany
B. Sonntag, Deutsches Elektronen-Synchrotron, Hamburg, Germany
Y. Hatano, Tokyo Inst. Tech., Tokyo, Japan
T. Sasaki, National Lab. for High Energy Physics, Ibaraki, Japan
H. Suzuki, Sophia University, Tokyo, Japan
H. P. Myers, Chalmers University of Technology, Gothenburg, Sweden